Evidence for Tissue-Specific JAK/STAT Target Genes in *Drosophila* Optic Lobe Development

Hongbin Wang, Xi Chen, Teng He, Yanna Zhou, and Hong Luo[1]
School of Life Sciences, Tsinghua University, Beijing 100084, China

ABSTRACT The evolutionarily conserved JAK/STAT pathway plays important roles in development and disease processes in humans. Although the signaling process has been well established, we know relatively little about what the relevant target genes are that mediate JAK/STAT activation during development. Here, we have used genome-wide microarrays to identify JAK/STAT targets in the optic lobes of the *Drosophila* brain and identified 47 genes that are positively regulated by JAK/STAT. About two-thirds of the genes encode proteins that have orthologs in humans. The STAT targets in the optic lobe appear to be different from the targets identified in other tissues, suggesting that JAK/STAT signaling may regulate different target genes in a tissue-specific manner. Functional analysis of *Nop56*, a cell-autonomous STAT target, revealed an essential role for this gene in the growth and proliferation of neuroepithelial stem cells in the optic lobe and an inhibitory role in lamina neurogenesis.

THE Janus kinase (JAK)/signal transducer and activator of transcription (STAT) pathway is highly conserved from invertebrates to vertebrates and plays important roles in a number of developmental processes, particularly in innate immune response, hematopoiesis, and growth control. JAK kinase hyperactivation is causally linked with leukemia and myeloproliferative disorders in humans (Lacronique *et al.* 1997; Constantinescu *et al.* 2008), while loss of JAK3 function leads to immunodeficiency (O'Shea *et al.* 2002). Originally identified in studies of interferon responses in mammalian cells, this pathway is activated by a large number of cytokines and growth factors (Levy and Darnell 2002). In the canonical model, the binding of a cytokine to its receptor causes dimerization of the receptor chains, which brings about close apposition of two associated JAK molecules leading to their activation through *trans*-phosphorylation. Activated JAKs phosphorylate STAT proteins on specific tyrosine residues, which then dimerize and translocate to the nucleus where they bind to specific DNA sequences and activate transcription of target genes. Although the signaling processes have been well studied, relatively little is known about how activation of this pathway is effected through the expression of target genes.

In *Drosophila*, this pathway consists of a complete but simpler set of components including three cytokine-like ligands, Unpaired (Upd), Upd2 and Upd3, a single receptor Domeless (Dome), a single JAK kinase Hopscotch (Hop), and a single STAT protein STAT92E (Arbouzova and Zeidler 2006). The JAK/STAT pathway plays a wide range of roles in *Drosophila* development, including embryonic segmentation, blood cell proliferation and differentiation, eye growth and polarity determination, heart development, border cell migration and stalk cell specification in the ovary, stem cell self-renewal in the testis and intestine, long-term memory formation, and circadian behavior (Arbouzova and Zeidler 2006; Jiang *et al.* 2009; Liu *et al.* 2010; Copf *et al.* 2011; Johnson *et al.* 2011; Xu *et al.* 2011; Luo and Sehgal 2012). Recent studies also indicated that the JAK/STAT pathway is required for the development of the larval optic lobe (Yasugi *et al.* 2008; Ngo *et al.* 2010; Wang *et al.* 2011a).

The optic lobe is the visual processing center of the *Drosophila* brain that contains several neuropils: the lamina, the medulla, the lobula, and the lobula plate (Figure 1, A and B; Meinertzhagen and Hanson 1993). The optic lobe derives from an embryonic optic placode (Green *et al.* 1993; Hofbauer and Campos-Ortega 1990). During early larval stages, the optic neuroepithelium undergoes extensive proliferation as two distinct populations: the outer proliferation center (OPC) and the inner proliferation center (IPC) (Figure 1A;

doi: 10.1534/genetics.113.155945
Manuscript received August 8, 2013; accepted for publication September 20, 2013; published Early Online September 27, 2013.
Supporting information is available online at http://www.genetics.org/lookup/suppl/doi:10.1534/genetics.113.155945/-/DC1.
[1]Corresponding author: School of Life Sciences, Tsinghua University, Beijing 100084, China. E-mail: luohong@mail.tsinghua.edu.cn; hongluo1010@gmail.com

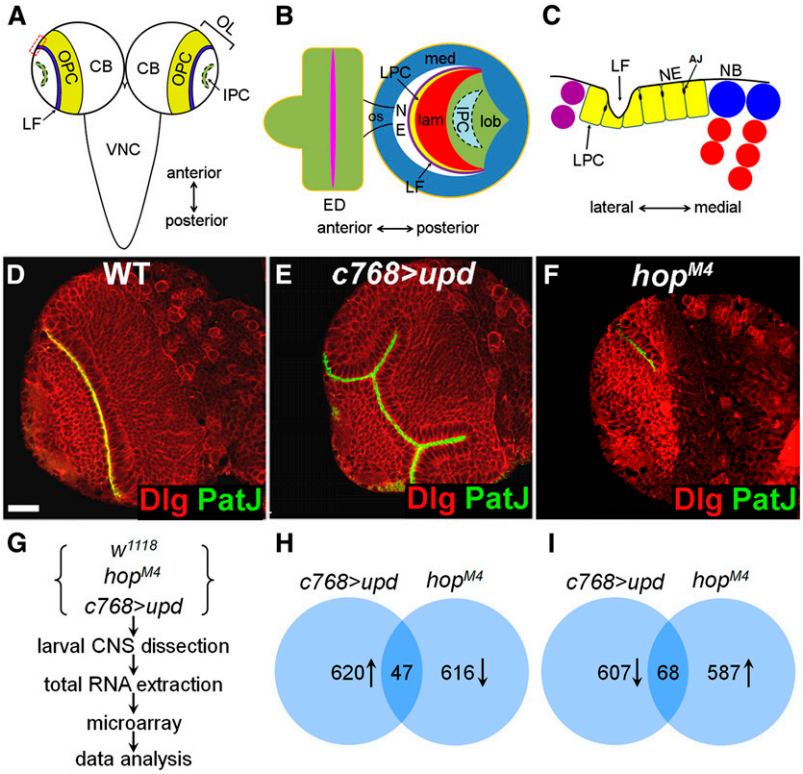

Figure 1 Identifying JAK/STAT target genes by microarrays. (A) The CNS consists of a pair of brain lobes and a ventral nerve cord (VNC). Each brain lobe is divided into central brain (CB) and laterally located optic lobe (OL) in which reside the outer proliferation center (OPC) and the inner proliferation center (IPC). (B) Lateral view of optic lobe showing the medulla (med), the lamina (lam), and the lobula complex (the lobula and the lobula plate) (lob). The eye disc (ED) is connected with the optic lobe through the optic stalk (os). (C) Magnified view of boxed region in A showing lamina and medulla neurogenesis on the lateral and the medial side of the OPC, respectively. LF, lamina furrow; LPC, lamina precursor cell; NE, neuroepithelial cell; NB, medulla neuroblast; AJ, adherens junction. (D–F) Brains dissected from late-third-instar larvae were stained with PatJ (green) and Dlg (red). (D) Wild-type brain; (E) *upd*-overexpressing brain; and (F) hop^{M4} brain. Frontal view, lateral is to the left and medial to the right. Scale bar: 20 μm for D–F. (G–I) The microarray assays. (G) Flowchart of microarray experiments. (H) Genes that are upregulated in *upd*-overexpressing brains but down regulated in hop^{M4} brains. (I) Genes that are downregulated in *upd*-overexpresing brains but upregulated in hop^{M4} brains.

Hofbauer and Campos-Ortega 1990). Lamina neurogenesis begins in the mid-third instar, on the lateral side of the OPC where retinal axon-delivered signals induce lamina precursor cells (LPCs) to divide once, generating postmitotic cells that differentiate into lamina neurons (Figure 1C; Kunes 2000). Medulla neurogenesis, on the other hand, starts in the late-second instar when neuroepithelial cells (NEs) on the medial edge of the OPC differentiate into neuroblasts (NBs), which undergo asymmetric division producing a daughter neuroblast that self-renews, and a smaller ganglion mother cell (GMC) that divides once producing two medulla neurons (Figure 1C; Nassif *et al.* 2003; Egger *et al.* 2007; Hayden *et al.* 2007). The maintenance of neuroepithelial stem cells and their differentiation into asymmetrically dividing progenitors must be tightly regulated. In JAK mutant brains, the NEs cannot be maintained and prematurely differentiate into medulla NBs, resulting in severe defects in lamina and medulla development (Yasugi *et al.* 2008; Ngo *et al.* 2010; Wang *et al.* 2011a). It is not well understood how the JAK/STAT pathway regulates neuroepithelial maintenance/expansion and the differentiation from NE to NB. To gain further insight into the roles of JAK/STAT in *Drosophila* brain development, we have attempted to identify JAK/STAT targets in the larval brain. We performed microarray analyses of genes that are differentially expressed in JAK/STAT mutant brains as compared with wild type and identified 47 targets positively regulated by JAK/STAT. More than 60% of these genes encode proteins highly conserved in humans. We further demonstrate that *Nop56* is a cell-autonomous STAT92E target and is required for neuroepithelial growth and negatively regulates lamina neurogenesis.

Materials and Methods

Fly strains and genetic crosses

Flies were reared on standard cornmeal food at 25° unless otherwise indicated. w^{1118} was used as a wild-type strain. The following alleles and transgenic lines used are described in FlyBase: hop^{M4}, $Nop56^{G4900}$, *UAS-upd*, $UAS\text{-}hop^{Tum\text{-}l}$, $UAS\text{-}dome^{DN}$, *c768-Gal4*, *c855a-Gal4*, and *GMR-Gal4*. We also used *UAS-Nop56* (Murata *et al.* 2008), $UAS\text{-}Nop56^{RNAi}$ lines [Vienna *Drosophila* RNAi Center (VDRC) stocks 51775 and 52165, and National Institute of Genetics (NIG) stocks 13849R2 and 13849R3], $UAS\text{-}stat92E^{RNAi}$ (Tsinghua Stock Center, THU 0573), and $UAS\text{-}Fibrillarin^{RNAi}$ (VDRC 104372). The *10XSTAT92E-GFP* line, carrying five tandem repeats of a genomic fragment in the *SOCS36E* gene that contains two potential STAT92E binding sites, is a reporter of JAK/STAT activity (Bach *et al.* 2007).

For overexpression and RNAi experiments, *UAS* flies were crossed with *c768-Gal4*, *c855a-Gal4*, or *GMR-Gal4* flies, and the progeny were cultured at 25° or 31° until various larval stages before analyses. To induce flip-out clones (Struhl and Basler 1993), $UAS\text{-}Nop56^{RNAi}$ or $UAS\text{-}stat92E^{RNAi}$ females were crossed to *y w hsFlp1/Y*; *actin* $< y^{+} <$ *Gal4*, *UAS-nGFP* males; larval progeny were heat-shocked at 38° for 30 min at 48 hr after larval hatching (ALH) and then cultured at 25° until mid-late third (about 84 hr ALH) to late-third instar stages (96 hr ALH) before dissection.

To generate *Nop56* mosaic clones, *FRT82B Nop56^{G4900}/TM6B Tb* females were crossed with *y w hs Flp1/Y*; *FRT82B Ub-GFP/TM2* males. Larval progeny were subjected to a 1-hr heat shock at 38° at about 48 hr ALH to induce somatic recombination. Mid-late third and late-third instar larvae were dissected for analyses.

RNA preparations and microarray analyses

The central nervous system (CNS) consisting of the brain lobes and ventral nerve cord (VNC) was dissected from late-third instar larvae in PBS and stored in RNAlater (Ambion) at 4° until 250–300 CNS specimens were collected. Total RNA was then extracted using Trizol (Invitrogen) and further purified using RNAeasy (Qiagen). Biotin-labeled cRNAs were hybridized to the Affymetrix *Drosophila* genome 2.0 arrays according to manufacturer's recommendations. After hybridization, the arrays were scanned with Affymetrix Gene Array Scanner 3000, and the data sets were analyzed using Microarray Suite 5.0 (MAS 5.0). Two independent array assays were performed for each genotype to reduce false-positive signals. A cutoff of a 1.3-fold increase or decrease in expression was used to identify genes that had differential expression in the mutant brains as compared with wild type.

In situ hybridization

Larval CNS was dissected from late-third instar larvae in PBS and fixed overnight at 4° with 8% paraformaldehyde in PBS containing 0.3% Triton X-100. Standard protocols for *in situ* hybridization were used (Tautz and Pfeifle 1989). Digoxigenin-labeled antisense probes were made for the following 25 genes: *CG1732*, *CG8772*, *CG8965*, *CG10376*, *CG14434*, *CG15220*, *CG32634*, *CG33275*, *CG33494*, *CR42862*, *Chromatin accessibility complex 16kD protein* (*Chrac-16*), *Enhancer of Polycomb* [*E(Pc)*], *E(spl) mδ*, *E(spl)m7*, *Female sterile (2) Ketel* [*Fs(2)Ket*], *glial cells missing* (*gcm*), *Hairless* (*H*), *Juvenile hormone epoxide hydrolase 2* (*Jheh2*), *Nop56*, *O/E-associated zinc finger protein* (*Oaz*), *Replication factor C subunit 4* (*RfC4*), *sulfateless* (*sfl*), *Twin of m4* (*Tom*), *Trehalase* (*Treh*), and *vielfaltig* (*vfl*).

Antibody production

The entire coding sequence of *Nop56* was amplified by PCR using *Drosophila* genomic DNA as template and the following primer set 5′-TTGCGGCCGCTCGGCATATATTCGGCA TAG-3′ and 5′-CCCTCGAGATCAGGGGGTCAAAGGAAAT-3′, with the underlying sequences added to facilitate cloning. The amplified PCR product was cloned into the bacterial expression vector pET28a. The protein was expressed by induction with 0.1 mM IPTG for 16 hr at 18°. Soluble protein fractions containing Nop56 were purified using a nickel column and used to immunize guinea pig. The anti-sera obtained were preadsorbed with fixed embryos and larval CNS specimens and then used to detect Nop56 protein expression.

Immunohistochemistry, BrdU labeling, and TUNEL assays

Larval brain staining was performed as previously described (Wang *et al.* 2011b). The following primary antibodies were used: guinea pig anti-Deadpan (1:1000, gift from J. Skeath), guinea pig anti-Miranda (1:500, gift from C. Doe), rabbit anti-PatJ (1:1000, gift from H. Bellen), guinea pig anti-Nop56 (1:100, this study), rabbit anti-SOCS36E (1:1000, gift from S. Hou), rabbit anti-PTP61F (1:100, gift from L. Rabinow), rabbit anti-Zfh-1 (1:100, gift from R. Lehmann), mouse anti-Discs large [1:100, Developmental Studies Hybridoma Bank (DSHB)], mouse anti-Dachshund (1:100, DSHB), rat anti-Elav (1:100, DSHB), mouse anti-Prospero (1:100, DSHB), rabbit anti-DE-Cadherin (sc-33743, 1:100, Santa Cruz Biotechnology), mouse anti-Fibrillarin (ab4566-250, 1:200, Abcam), and rat anti-BrdU (1:100, Abcam). Secondary antibodies used were: Alexa Fluo-488 goat anti-rabbit (1:200) and Alexa Fluo-488 goat anti-rat (1:200) (Molecular Probes); Cy3-conjugated goat anti-mouse (1:200), Cy3-conjugated goat anti-rat (1:200), Cy5-conjugated goat anti-rat (1:200), and Cy5-conjugated donkey anti-guinea pig (1:200) (Jackson ImmunoResearch Lab).

For BrdU labeling, brains were dissected from mid-third instar larvae in Schneider *Drosophila* medium, incubated in 200 μg/ml BrdU in the medium for 1 hr at room temperature and then fixed as described above. Prior to incubation with anti-BrdU antibody, the brains were incubated in 2 N HCl for 30 min and neutralized by washing with 0.1 M boric acid. A TUNEL assay kit (Millipore no. S7165) was used to detect apoptotic cells in larval brains. Confocal images were acquired by an Olympus FV500 confocal microscope (60× objective, N.A.1.4) and a Nikon A1R MP confocal microscope [60× (WI) objective, N.A.1.27], and processed using Imaris (Bitplane) and Adobe Photoshop 7.0 software.

Results

Whole-genome analyses of JAK/STAT targets in the Drosophila brain

The JAK/STAT pathway is active in the optic lobe (Yasugi *et al.* 2008; Ngo *et al.* 2010; Wang *et al.* 2011a). Overexpression of *upd* or *hop$^{Tum\text{-}l}$*, which encodes an activated JAK kinase (Harrison *et al.* 1995; Luo *et al.* 1995), results in neuroepithelial overgrowth whereas loss of *hop* activity leads to an early depletion of NEs and a small brain lobe (Figure 1, E and F; Wang *et al.* 2011a). The JAK/STAT pathway appears to be specifically required in the optic lobe, as loss of JAK/STAT function has no effect on central brain or ventral nerve cord development (Wang *et al.* 2011a). To obtain a genome-wide survey of JAK/STAT targets in the brain, we isolated total RNA from the CNS of wild-type, hemizygous *hop^{M4}*, and *upd*-overexpressing late-third instar larvae cultured at 25° and conducted microarray assays using Affymetrix oligonucleotide array chips representing about 13,600 annotated *Drosophila* genes.

Table 1 Genes positively regulated by JAK/STAT

Probe Set ID	Gene Name	FC oe/wt	FC lof/wt	Function	Human Homolog	SB Sites	Conserved SBS	Reported Target
1628052_at	Cyp6a17	3.5	−6.3	Cytochrome P450, electron transport	CYP5A1			
1638568_s_at	H	3.3	−1.5	Transcription corepressor		2/434	Yes	
1628238_at	Tektin-C	3.3	−7	Microtubule cytoskeleton organization	TEKT1			
1640821_at	ftz-f1	2.6	−1.3	Zinc finger transcription factor	NR5A2	2/359	Yes	
1628689_at	CG17211	2.5	−2.6	Unknown				
1635692_s_at	Treh	2.4	−1.3	Trehalase activity	TREH	3/228	Yes	
1635766_at	Fs(2)Ket	2.4	−1.7	Protein import into nucleus	KPNB1	2/342	Yes	
1633334_at	CG15822	2.3	−1.7	Unknown	KALRN	4/981	Yes	
1637631_at	tutl	2.2	−1.9	Axon guidance, signal transduction	IGSF9B	2/379	Yes	
1633033_s_at	CG1732	2.2	−1.5	Neurotransmitter transport	SLC6A1	3/186		
1628411_at	Oaz	2.1	−2.6	Zinc finger transcription factor	ZNF423	4/993	Yes	
1623256_at	GstE1	2.1	−7.2	Glutathione transferase activity				
1629181_at	CG33494	2.1	−1.8	Unknown		3/414		
1639074_at	CG33275	2	−1.8	Guanyl-nucleotide exchange factor	PLEKHG4	3/773		
1633109_at	CG33229	2	−29.9	Unknown				
1626553_at	CG10376	2	−1.5	Protein serine/threonine phosphatase	PPM1F	2/670		
1637900_at	CG11852	1.9	−1.6	Hormone binding, odorant binding protein		2/411		
1633591_at	gcm2	1.9	−2.6	Transcription factor	GCM2			
1634658_a_at	CG8772	1.8	−1.3	Glutaminase activity	GLS	2/961	Yes	
1628110_s_at	E(Pc)	1.8	−1.5	Maintenance of chromatin architecture	EPC1			
1626233_at	CG8965	1.8	−2.2	Signal transduction		2/428		Up[a]
1625530_at	CG10462	1.8	−1.7	Zinc finger transcription factor				Up[b]
1624345_a_at	Nop56	1.8	−1.3	rRNA metabolism	NOP56	2/564		
1641174_at	RFeSP	1.8	−3.9	Ubiquinol-cytochrome-c reductase activity	UQCRF1			
1637610_at	Chrac-16	1.7	−1.7	Chromatin accessibility complex	CHRAC-1	2/444	Yes	Down[b]
1638370_s_at	vfl	1.7	−1.6	Zinc finger transcription factor		2/208	Yes	
1635089_at	tun	1.7	−1.6	Hydrolase activity	WDYHV1			Up[b]
1633451_at	CG32634	1.7	−2.7	Unknown				
1629940_at	CG13895	1.7	−1.6	Centromere protein Cenp-B	TIGD3			
1631126_at	gcm	1.6	−2.2	Transcription factor	GCM1			
1625116_at	trol	1.6	−1.4	Extracellular matrix protein	HSPG2	2/165		Up[a, b]
1629523_at	lola	1.6	−1.6	Zinc finger transcription factor		2/188		Up[b]
1631534_at	sfl	1.6	−1.5	Sulfotransferase activity	NDST2	2/522		Down[b]
1624881_at	CG11448	1.6	−28.3	Protein binding	RILPL1	2/937		
1624476_at	Tom	1.5	−1.4	Target of Notch signaling		3/71	Yes	
1625493_at	E(spl)m7	1.5	−1.6	Target of Notch signaling	HES1	2/503		
1631048_at	CG14434	1.5	−1.4	Unknown				
1631363_at	Nuf2	1.5	−1.5	Kinetochore protein		2/147		
1635936_at	CG13822	1.5	−3.8	Protein binding	GILT	2/510		Down[b]
1634011_at	E(spl)mδ	1.5	−1.4	Target of Notch signaling				
1634199_at	CG15220	1.5	−1.4	DNA replication factor A complex	RPA3			
1626996_s_at	br	1.5	−1.5	Zinc finger transcription factor		2/604		Up[a]
1627773_a_at	Jheh2	1.4	−1.3	Juvenile hormone epoxide hydrolase	EPHX1	2/257	Yes	
1634943_at	RfC4	1.4	−1.5	DNA replication factor C complex	RFC2			
1641102_at	CG14141	1.4	−1.5	Unknown	PTPRD			
1628318_at	Spc105R	1.4	−1.4	Kinetochore assembly	Spc105	2/515		
1625672_s_at	CR42862	1.4	−1.6	Noncoding RNA				

FC, fold change; wt, wild type; oe, *upd* overexpression; lof, hop^{M4}; SB Sites, STAT92E binding sites, the numbers refer to the number of STAT92E binding sites in the no. of base pairs of DNA sequence; Conserved SBS, STAT92E binding sites found in other *Drosophila* species, indicated by "Yes." Up, positive regulation by JAK/STAT; Down, negative regulation by JAK/STAT.

[a] Terry *et al.* (2006).

[b] Flaherty *et al.* (2009).

Compared with wild type, 620 genes were upregulated in JAK activated (*upd*-overexpressing) brains (Figure 1H and Supporting Information, Table S1), and an almost equal number of genes (607) were downregulated (Figure 1I and Table S1). By contrast, in JAK-inactivated (hop^{M4}) brains, 616 genes were downregulated, and 587 genes were upregulated (Figure 1, H and I, and Table S2). Thus, it appears that JAK/STAT signaling not only activates gene expression but also represses a large number of genes.

We expected that positively regulated genes would have increased, decreased expression in JAK activated, and JAK inactivated brains, respectively, whereas negatively regulated genes would have opposite changes in expression. Using these criteria, we identified 47 positively regulated

Table 2 Genes negatively regulated by JAK/STAT

Probe Set ID	Gene Name	FC oe/wt	FC lof/wt	Function	Human Homolog	SB Sites	Conserved SBS	Reported Target
1640035_at	Fbp2	−57.7	2.9	lipid metabolism	FBP2			
1638338_a_at	Fbp1	−22.2	2.7	protein transporter	FBP1			
1635689_at	Lcp2	−21.1	1.9	structural constituent of larval cuticle	LCP2			
1623675_at	Obp99b	−20.7	1.7	odorant binding protein				
1626830_at	Lcp1	−8	3.5	structural constituent of larval cuticle	LCP1			
1626429_at	Lsp1	−7	2.7	oxygen transporter	LSP1			
1628699_at	Lsp1	−7	2.1	oxygen transporter	LSP1			
1638108_at	Sgs8	−6.7	13.9	structural molecule activity, puparial adhesion		4/993	Yes	
1634409_at	CG31775	−6	1.7	unknown				
1641070_at	CG9021	−5.9	1.5	protein binding		4/629		
1626088_at	CG2177	−5.5	3.1	metal ion transporter	SLC39A9			Up[a]
1626910_at	CG15282	−5.2	2.7	unknown		2/705		
1634997_at	Sgs5	−5	15.5	puparial adhesion				
1632529_at	tinc	−4.6	1.5	eye photoreceptor cell development		2/278		
1629106_at	CG2233	−4.5	2	unknown				
1627946_at	CG12068	−4	2.1	visual perception	HSD17B6			
1635549_at	TotA	−3.8	2.7	regulation of translation		3/146		
1633607_at	CG2444	−3.7	1.8	unknown				
1630238_at	Lcp4	−3.5	1.7	unknown		4/596		
1635548_s_at	CG15281	−3.5	2.1	unknown				
1631701_a_at	CG8502	−3.4	1.6	structural constituent of larval cuticle	ATP1B2			
1637552_s_at	CG32423	−3	1.7	mRNA processing	RBMS1	2/102		
1627219_at	nAcR64B	−3	1.5	cation transport	CHRNA4			
1630593_at	NLaz	−2.9	1.9	lipid transport	APOD			Down[a]
1641634_at	Lsp2	−2.8	2.1	transport				
1630635_s_at	CG7720	−2.8	2	cation transporter activity	SLC5A8	3/511		Down[a]
1631059_at	Pkc98E	−2.7	1.8	protein serine/threonine kinase activity	PRKCE	2/183		
1634525_at	CG7738	−2.6	3.6	protein binding		2/735		
1638789_at	fau	−2.6	1.8	protein binding	FAU			
1638314_at	CG12418	−2.6	1.7	unknown				
1625880_at	CG17618	−2.6	1.4	maintenance of cell polarity				
1629229_a_at	srp	−2.4	1.9	transcription factor	GATA6	2/542		
1632121_a_at	CG6416	−2.4	1.6	mesoderm development		3/479		
1624211_at	CG9005	−2.4	1.4	unknown	FAM214			
1634012_at	CG5002	−2.3	1.9	anion transport	SLC26A11	3/254	Yes	
1625236_s_at	Prosap	−2.3	1.4	protein binding		3/354	Yes	Down[a]
1634447_at	CG31140	−2.2	1.4	diacylglycerol kinase activity	DGKH			
1636835_at	CG16700	−2.2	1.3	amino acid transport	SLC36A4			Up[a]
1632431_s_at	Ance	−2.1	2.1	proteolysis,peptidyl-dipeptidase A activity	ACE			Down[a]
1628005_at	CG31666/ chinmo	−2.1	1.4	zinc finger transcription factor	BTBD10	2/219		Up[a,b]
1633048_at	CG8193	−2.1	1.4	transport				
1638899_s_at	CG15312	−2.1	1.3	unknown	CNTN2	2/520		
1639079_at	Adgf-D	−2	1.6	adenosine deaminase activity, cell proliferation	CECR1	2/910	Yes	
1624686_a_at	dnc	−2	1.4	3′,5′-cyclic-AMP phosphodiesterase	PDE4D	4/985	Yes	
1634552_at	TepIV	−2	1.3	endopeptidase inhibitor activity		4/785		
1630095_a_at	Drl-2	−1.9	1.8	transmembrane receptor protein tyrosine kinase	RYK	4/764		
1625967_s_at	l(3)10615	−1.9	1.5	unknown				
1629889_s_at	regucalcin	−1.9	1.4	calcium-mediated signaling		2/829	Yes	
1631554_at	CG11473	−1.9	1.4	unknown				
1624363_at	CG15201	−1.8	2.7	unknown	RGN			
1627242_at	l(2)efl	−1.8	2.7	protein folding	CRYAB			
1626842_a_at	l(3)82Fd	−1.8	1.6	cell wall catabolism	NCOA7	2/427	Yes	
1638820_at	CG12870	−1.8	1.6	apoptosis		2/236		
1628757_at	Glut1	−1.7	6	glucose transporter activity	SLC2A1			
1626113_at	CG4080	−1.7	2.3	ubiquitin cycle, zinc finger	C3HC4	2/454		
1636313_at	CG4914	−1.7	2.1	transcription factor	TMPRSS11B			Down[a]

(continued)

Table 2, *continued*

Probe Set ID	Gene Name	FC oe/wt	FC lof/wt	Function	Human Homolog	SB Sites	Conserved SBS	Reported Target
1639320_a_at	Ddc	−1.7	1.9	catecholamine metabolism	DDC			
1631215_at	CG32132	−1.7	1.8	unknown				
1636103_a_at	nocturnin	−1.7	1.7	nucleic acid binding	CCRN4L	2/322		
1625462_s_at	CG31221	−1.7	1.4	lipoprotein receptor activity	BRCA2	2/98		
1639826_at	CG32662	−1.7	1.4	unknown	GOLGA6L10	2/64		
1640729_s_at	nrv3	−1.7	1.4	potassium ion transport		2/620		
1633592_a_at	CREG	−1.6	2.2	transcriptional repressor activity	CREG1	2/310		
1628632_at	Paip2	−1.6	1.4	negative regulation of translation	PAIP2	2/275		
1627151_at	CG4612	−1.6	1.3	mRNA binding	PABPN1			
1626417_at	Cht3	−1.4	1.5	chitinase activity	CHIA	3/621		
1626272_s_at	CG3066	−1.4	1.3	serine carboxypeptidase				
1636122_at	Socs16D	−1.4	1.3	signal transduction	SOCS7			

FC, fold change; wt, wild type; oe, *upd* overexpression; lof, hop^{M4}; SB Sites, STAT92E binding sites, the numbers refer to the number of STAT92E binding sites in the number of base pairs of DNA sequence; Conserved SBS, STAT92E binding sites found in other *Drosophila* species, indicated by "Yes." Up, positive regulation by JAK/STAT; Down, negative regulation by JAK/STAT.

[a] Flaherty *et al.* (2009).

[b] Terry *et al.* (2006).

(Figure 1H and Table 1) and 68 negatively regulated genes (Figure 1I and Table 2). In the studies presented below, we focused on the positively regulated genes.

Verification of target gene expression in the brain

In situ hybridization assays were performed for 25 positively regulated genes. We found that 24 of them are expressed in the optic lobe with specific patterns (Figure 2), while *sfl* has a ubiquitous, low level of expression in the optic lobe (not shown). These 24 genes can be grouped into four classes: (1) class I genes are expressed in the NEs, including *CG1732*, *CG14434*, *CG15220*, *CG32634*, *CR42862*, *Chrac-16*, *E(Pc)*, *H*, *Nop56*, *RfC4*, *Treh*, and *vfl* (Figure 2, A–L); (2) class II genes are expressed in LPCs (Figure 2, M–Q), including *CG8772*, *Fs(2)Ket*, *Jheh-2*, and *Tom*, which are expressed in discrete groups of cells, and *gcm*, which is expressed in a continuous stretch of cells; (3) class III genes are expressed in mature lamina neurons, including *CG8965*, *CG10376*, *CG33494*, *E(spl)mδ*, *E(spl)m7*, and *Oaz* (Figure 2, R–W); and (4) class IV gene, *CG33275*, is expressed in developing lamina neurons and the IPC (Figure 2X). Each of these genes was upregulated in JAK-activated brains, but was strongly reduced or undetectable in JAK-inactivated brains (Figure 2). These results are consistent with the microarray data (Table 1) and validate our approach to identifying JAK/STAT target genes.

To examine which genes might be direct STAT92E targets, we searched for putative enhancers with STAT92E binding site clusters from 5 kb upstream to 5 kb downstream of each gene. *In vitro* studies showed that STAT92E binds to the consensus sequence TTCNNNGAA (Yan *et al.* 1996), which is similar to mammalian STAT binding sites. Twenty-eight genes (60%) that have at least two STAT92E binding sites in a short noncoding genomic sequence were identified (Table 1). Further, the STAT92E binding site clusters in 12 genes are conserved in diverse *Drosophila* species (Table 1), increasing the possibility that these sites are activated by STAT92E. In comparison, a similar search for 40 randomly selected genes identified only four genes (10%) with STAT92E binding site clusters (data not shown).

Interestingly, nearly half of the negatively regulated genes (31/68) also contain clusters of STAT92E binding sites (Table 2), suggesting that these genes may be directly repressed by activated STAT92E. While not extensively studied, the repressor function of STAT protein has been reported in the slime mold *Dictyostelium* (Mohanty *et al.* 1999).

Nop56 is a functional target of JAK/STAT signaling

We examined in more detail the relationship between JAK/STAT signaling and *Nop56*, a potential direct target gene. *Nop56* encodes a protein highly conserved from yeast to humans. In the yeast, it is involved in ribosome biogenesis and cell growth (Gautier *et al.* 1997). The role of *Nop56* in animal development has not been well studied. Previous studies showed that *Nop56* gene expression is activated by dMyc, implicating Nop56 in cellular growth in *Drosophila* (Orian *et al.* 2003; Hulf *et al.* 2005; Pierce *et al.* 2008; Furrer *et al.* 2010). Neumüller *et al.* (2011), through RNA interference (RNAi) screens, identified *Nop56* as a regulator of neuroblast proliferation in the central brain.

Nop56 RNA is detected in the NEs (Figure 2I1), and its expression positively responds to JAK signaling activity (Figure 2I2, I3). We raised an antibody to study Nop56 protein expression and found that the protein is strongly expressed in the NEs, medulla neuroblasts, LPCs, and the IPC (Figure 3, A and B) and in neuroblasts of the central brain and VNC (not shown). Nop56 expression is much reduced in lamina and medulla neurons (Figure 3A). Costaining with Fibrillarin, a marker for the nucleolus, showed that Nop56 is localized in the nucleolus (Figure 3C). The specificity of this antibody can be demonstrated by the strong reduction or loss of Nop56 protein in NE clones expressing $Nop56^{RNAi}$ (Figure 3D). Importantly, Nop56

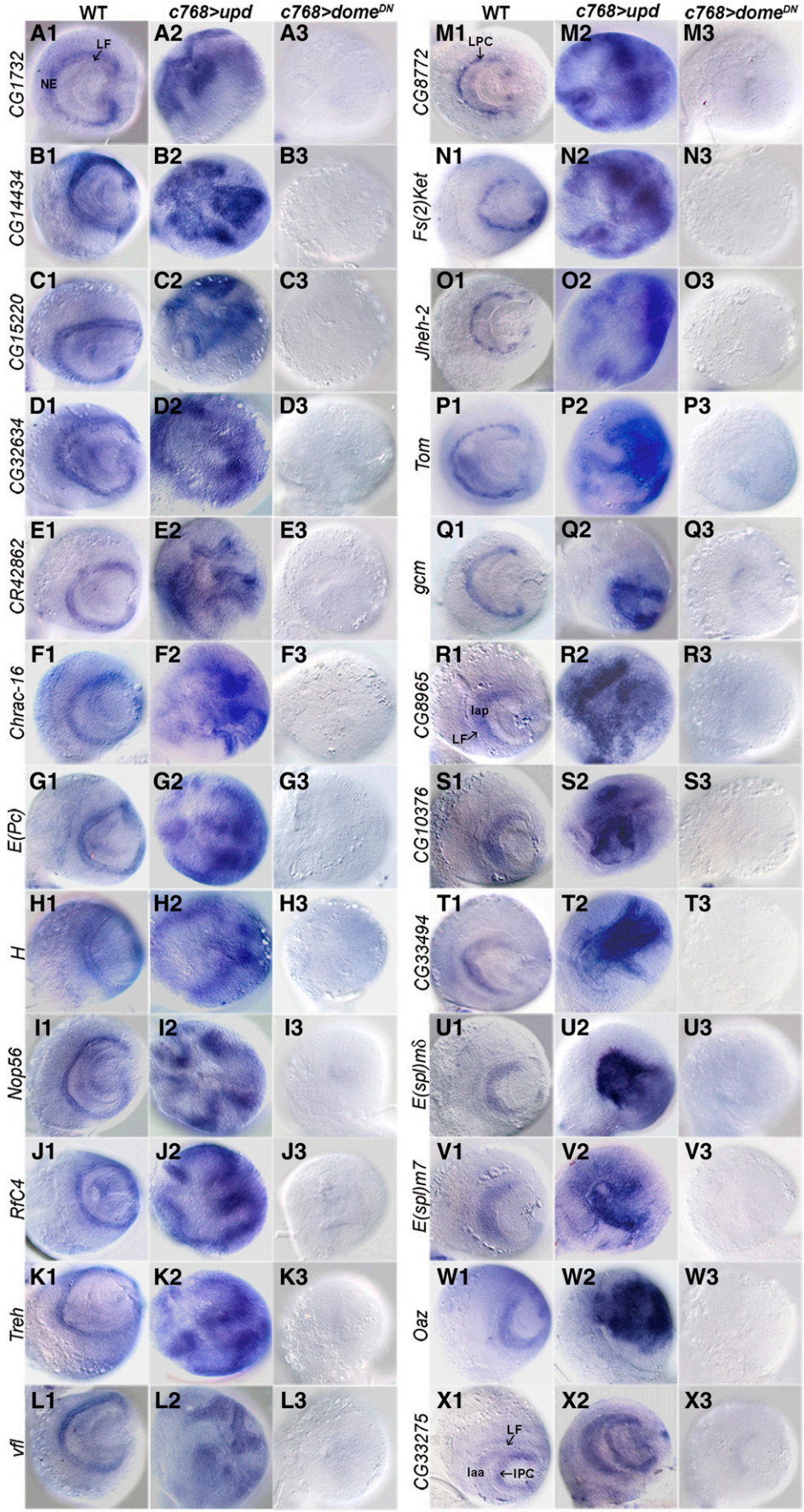

Figure 2 Verification of JAK/STAT targets by *in situ* hybridization. (A–L) Targets expressed in the NEs. (M–Q) Targets expressed in LPCs. (R–W) Targets expressed in mature lamina neurons. (X) *CG33275* expressed in developing lamina neurons and the IPC. Each gene was upregulated in brains overexpressing *upd* and downregulated in brains expressing a dominant-negative Dome receptor (*dome*^{DN}). NE, neuroepithelial cells; LF, lamina furrow; LPC, lamina precursor cell; laa, anterior lamina cells (developing lamina neurons); lap, posterior lamina cells (mature lamina neurons). Lateral view, anterior is to the left and dorsal is up.

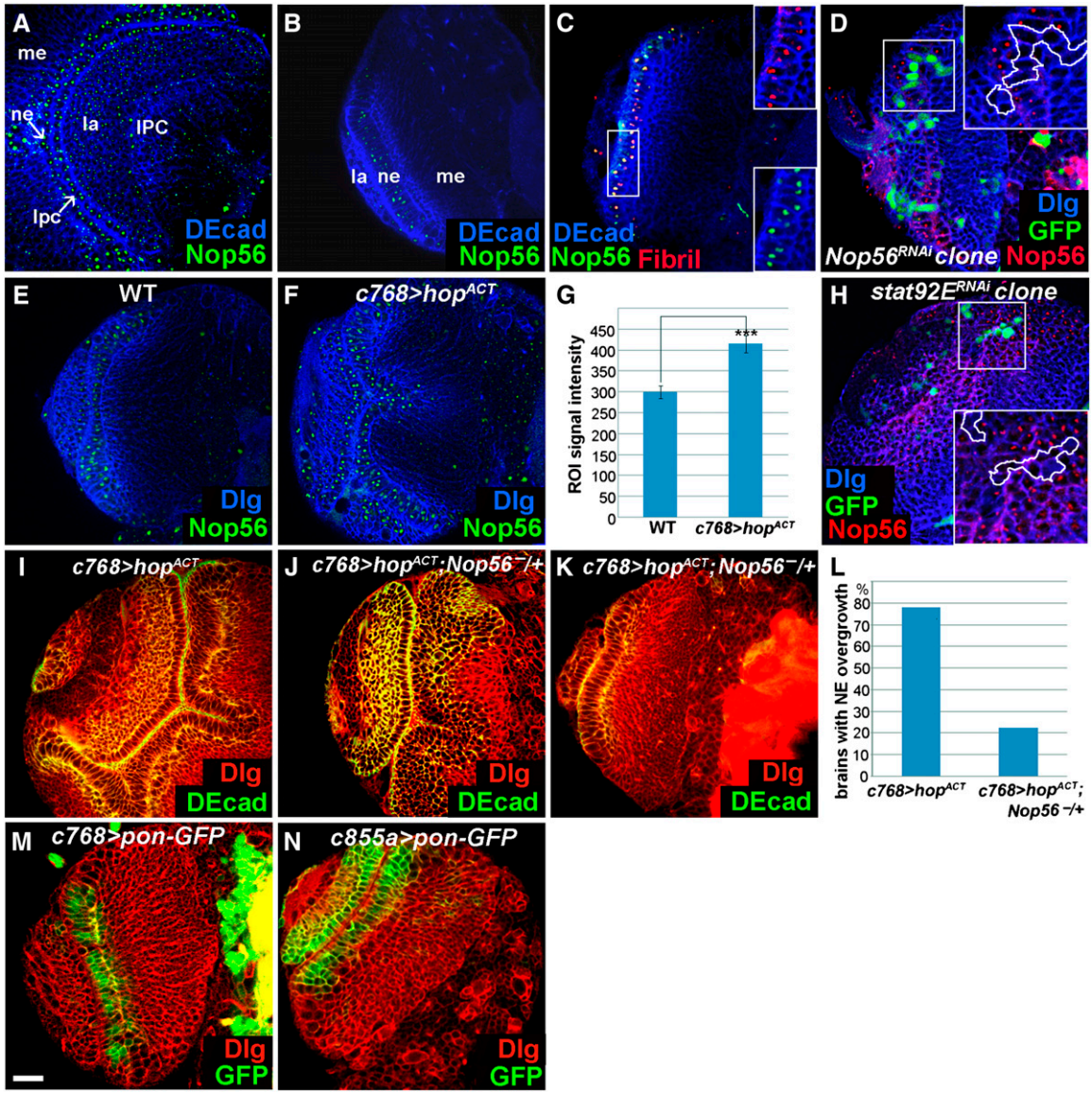

Figure 3 *Nop56* is a functional target of the JAK/STAT pathway. Brains dissected from mid-late third- and late-third-instar larvae cultured at 25° were stained with the makers indicated. (A and B) Nop56 protein is strongly expressed in the NEs, medulla neuroblasts, LPCs, and the IPC, but is weakly expressed in lamina and medulla neurons. ne, neuroepithelial cells; lpc, lamina precursor cell; me, medulla; la, lamina; IPC, inner proliferation center. (C) Nop56 protein colocalizes with Fibrillarin (Fibril). (D) Nop56 expression is reduced or eliminated in clones of cells expressing $Nop56^{RNAi}$. (E–G) Nop56 level increases in the NEs overexpressing hop^{ACT} (*c768–Gal4/UAS–*$hop^{Tum\text{-}l}$) (F), as compared with wild type (E); (G) quantification of Nop56 staining intensity, $n = 17$ ROIs (region of interests) for wild-type and for *c768–Gal4/UAS–*$hop^{Tum\text{-}l}$ brains, each ROI contains 50 nucleoli. ***, $P < 0.01$. (H) Nop56 expression is reduced or eliminated in clones of cells expressing $stat92E^{RNAi}$. (I–L) Overexpression of $hop^{Tum\text{-}l}$ causes neuroepithelial overgrowth (I), a reduction of *Nop56* gene dosage to half ($Nop56^{G4900}$/+), partially (J), or almost completely (K) suppressed neuroepithelial overgrowth; (L) quantification of suppression: 78% of *c768–Gal4/UAS-*$hop^{Tum\text{-}l}$ brains ($n = 23$) had neuroepithelial overgrowth; only 22% of *c768–Gal4/UAS-*$hop^{Tum\text{-}l}$; $Nop56^{G4900}$/+ brains ($n = 36$) still had significant neuroepithelial overgrowth. (M and N) Expression patterns of *c768–Gal4* and *c855a–Gal4* as revealed by *UAS–pon–GFP*. (A) Lateral view, anterior is to the left, dorsal is up; (B–F, H–K, M, and N) frontal view, lateral is to the left, medial to the right. Scale bar, 20 μm.

protein expression increased in the NEs overexpressing $hop^{Tum\text{-}l}$ (Figure 3, E–G, compare F with E; quantification is shown in G), and was strongly reduced or eliminated cell autonomously in clones of NEs expressing $stat92E^{RNAi}$ (Figure 3H). A reduction of *Nop56* gene dosage to half ($Nop56^{G4900}$/+) significantly suppressed neuroepithelial overgrowth of JAK-activated brains (Figure 3, I–L), indicating that Nop56 is an important mediator of JAK/STAT activation in the optic lobe.

Nop56 is required for neuroepithelial growth in the optic lobe

To study the role of *Nop56* in optic lobe development, we used RNAi to knock down *Nop56* expression, using

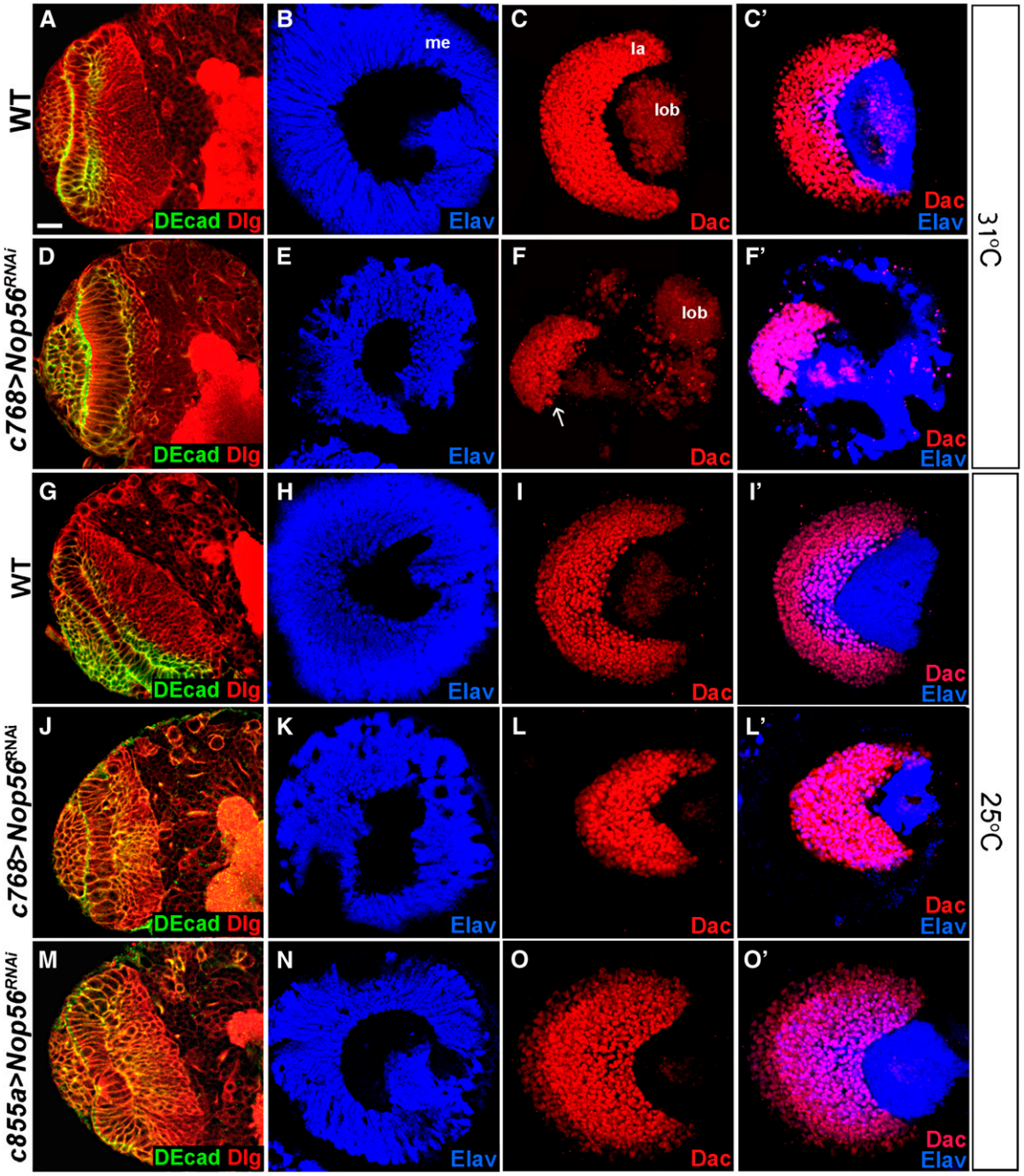

Figure 4 *Nop56* is essential for optic lobe development. (A–F′) Brains dissected from late-third-instar larvae cultured at 31° were stained with the makers indicated. (A–C′) Wild-type optic lobes having columnar NEs (A), a dome shaped medulla cortex (B), and a crescent lamina (C, C′). me, medulla; la, lamina; lob, lobula complex. (D–F′) *c768–Gal4/UAS-Nop56*^{RNAi} optic lobes having elongated NEs (D), a small medulla cortex (E), and a small, truncated lamina (F, F′; arrow indicates lamina). Note that all lamina cells differentiated into mature neurons (F′). (G–O′) Brains dissected from late-third-instar larvae cultured at 25° were stained with the markers indicated. (G–I′) Wild-type optic lobes having columnar NEs (G), a dome-shaped medulla cortex (H), and a crescent lamina (I and I′). (J–L′) *c768–Gal4/UAS–Nop56*^{RNAi} optic lobes having elongated NEs (J), a smaller medulla (K), and a smaller lamina (L) in which all cells differentiated into mature lamina neurons (L′). (M–O′) *c855a–Gal4/UAS–Nop56*^{RNAi} optic lobes having elongated NEs (M), a smaller medulla (N), but an enlarged lamina (O) in which more lamina cells differentiated into mature neurons (O′, compare with I′). (A, D, G, J, M) Frontal view, lateral is to the left, medial to the right; (B–C′, E–F′, H–I′, K–L′, N–O′) lateral view, anterior is to the left, dorsal is up. Scale bar, 20 μm.

c768–Gal4, a driver active in the NEs from the first-instar stage onward (Figure 3M; Wang *et al.* 2011b). Knockdown of *Nop56* RNA at 31° caused severe optic lobe defects. The medulla was much reduced in size (Figure 4E; 97%, n = 36), and the lamina had only small patches of cells (Figure 4F; 100%, n = 36). Knockdown of *Nop56* RNA at 25° led to similar but less severe defects in medulla and lamina development (Figure 4, K and L), which is expected

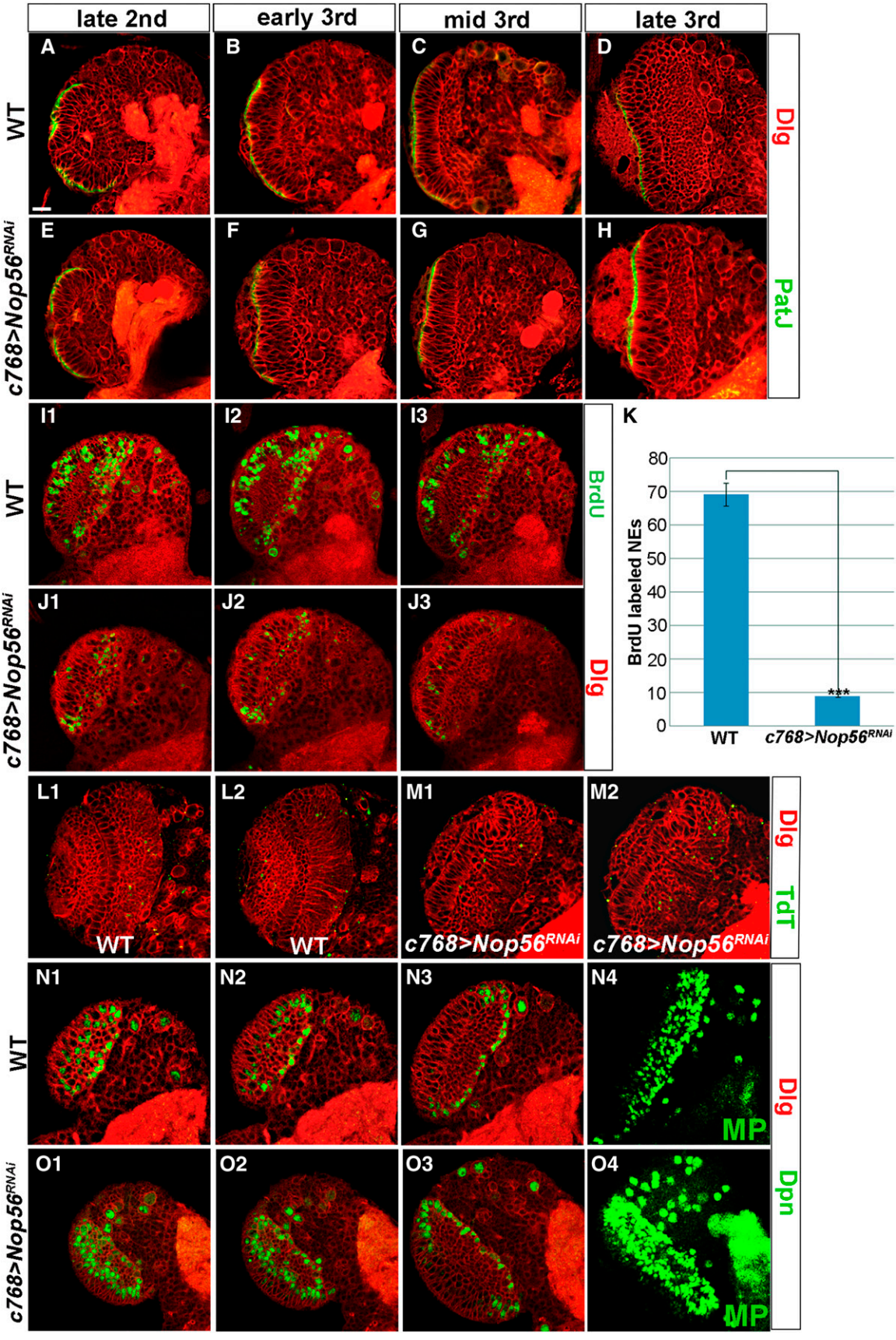
late 2nd
early 3rd
mid 3rd
late 3rd
WT
c768>Nop56RNAi
A
B
C
D
E
F
G
H
Dlg
PatJ
I1
I2
I3
J1
J2
J3
BrdU
Dlg
K
BrdU labeled NEs
80
70
60
50
40
30
20
10
0
***
WT
c768>Nop56RNAi
L1
L2
M1
M2
WT
WT
c768>Nop56RNAi
c768>Nop56RNAi
Dlg
TdT
N1
N2
N3
N4
O1
O2
O3
O4
MP
MP
Dlg
Dpn

because RNAi knockdown would be less efficient at lower temperature due to reduced Gal4 activity. To ascertain that the *Nop56* RNAi did not cause nonspecific effects, we expressed several additional *Nop56^{RNAi}* constructs, which together targeted two different regions of *Nop56* RNA; expression of these constructs led to similar optic lobe defects (Figure S1). The eye imaginal discs were not affected by *Nop56* RNAi under *c768–Gal4* control (Figure S2B), and knockdown of *Nop56* RNA using *GMR–Gal4*, which is active only in eye imaginal disc cells behind the morphogenetic furrow, did not cause defects in eye or lamina development (Figure S2D). Thus, the lamina defect did not arise from abnormal eye development. We conclude that *Nop56* activity is required for both lamina and medulla development.

Since the OPC generates precursor cells for lamina and medulla neurons, the defects observed in *Nop56* RNAi brains might arise from a deficiency in neuroepithelial maintenance and expansion in earlier larval stages. We thus performed a time-course study to examine whether neuroepithelial growth was affected by the loss of *Nop56* activity (Figure 5, A–H). The NEs can be recognized by staining for apical epithelial markers PatJ and atypical PKC (aPKC), adherens junction protein DE-cadherin, and basolateral marker Discs large (Dlg). In wild-type brains, the optic neuroepithelium grows during early larval stages and reaches a maximal size by mid-third instar; the NEs then gradually reduce in number as neurogenesis takes place on both the lateral and the medial side of the OPC (Figure 5, A–D). In brains expressing *Nop56^{RNAi}*, early neuroepithelial proliferation did not seem to be affected since the mutant brains had similar numbers of NEs to wild type till the late-second-instar stage (Figure 5E). However, the mutant NEs proliferated poorly subsequently and did not expand from the early third-instar stage onward (Figure 5, F–H); instead, the NEs became elongated, perhaps reflecting an increase in cell mass and volume (Figure 5, F–H; compare with C and D and see Figure 4D). To further examine the effect of *Nop56* loss on neuroepithelial proliferation, we performed BrdU labeling to monitor DNA replication in wild-type and *Nop56^{RNAi}* brains dissected from mid-third-instar larvae. We found that *Nop56* mutant NEs had much reduced BrdU labeling (Figure 5, J and K), suggesting that loss of *Nop56* inhibited cell-cycle progression. No significant cell death was detected in the mutant brains (Figure 5M). We conclude that *Nop56* activity is required for neuroepithelial growth, probably by affecting cell-cycle progression.

Loss of Nop56 leads to premature neuroepithelial differentiation into neuroblast

Cell-cycle progression is tightly linked with neuroepithelial maintenance and the transition from NE to NB (Zhou and Luo 2013). We therefore tested whether loss of *Nop56* might lead to premature neuroepithelial differentiation. Indeed, we found that while wild-type brains had a limited number of medulla NBs at mid-third instar (Figure 5, N1–N4), the number of NBs increased significantly in *Nop56^{RNAi}* brains (Figure 5, O1–O4).

To further examine the cell-autonomous requirement of *Nop56* in neuroepithelial maintenance, we removed *Nop56* activity in cell clones. Clones of cells expressing *Nop56^{RNAi}* were induced at late-second instar, and brains were examined at mid-late-third to late-third instar stages. NE clones were infrequently found, and most clones were entirely localized in the medulla cortex. The NE clones, when found, contained a few NEs and a number of cells in the medulla cortex (Figure 6A). Some mutant cells in the medulla expressed Dpn, indicating that they had prematurely differentiated into neuroblasts (Figure 6, A and B). The neuroblasts appeared to undergo asymmetric cell division as Miranda (Mira) was localized in a crescent at one pole during mitosis (Figure 6E). Prospero (Pros), which is weakly expressed in the GMCs but not in medulla neurons, was detected in a number of cells (Figure 6, G and I), suggesting that GMCs were generated. Mature neurons were also generated in the clone, as revealed by the expression of Elav, a neuron-specific marker (Figure 6G). Similarly, in mosaic clones mutant for a strong loss-of-function *Nop56* allele, *Nop56^{G4900}*, ectopic neuroblasts were generated; the clones were most frequently found in the medulla, presumably extruded from the neuroepithelium (Figure 6, C, D, and F). Taken together, these data indicate that *Nop56* is required for neuroepithelial growth/expansion, and loss of *Nop56* function in cell clones leads to premature differentiation of NEs into NBs, which can self-renew and generate medulla neurons.

Figure 5 *Nop56* is essential for neuroepithelial growth. (A–H) Brains dissected from larvae cultured at 25° were stained with PatJ (green) and Dlg (red). In wild-type brains (A–D), NE numbers per brain section increased from 42 at early third-instar to 71 at mid-third instar and then dropped to 60 at late-third instar, whereas in *c768–Gal4/UAS–Nop56^{RNAi}* brains (E–H), NE numbers did not change from early third to late-third-instar stages, averaging about 29 cells, but the mutant NEs became elongated in the third-instar stages (F, G, H, compare with C and D). (I–K) BrdU labeling of brains dissected from mid-third-instar larvae cultured at 25°. Three brain sections at comparable levels were shown for wild-type (I1, I2, I3) and *c768–Gal4/UAS–Nop56^{RNAi}* brains (J1, J2, J3); (K) quantification of BrdU labeling, the total number of labeled NEs in three sections was used for calculation. *Nop56* RNAi brains had a much reduced number of labeled NEs (n = 10 for wild-type and for *Nop56* RNAi brains; ***, $P < 0.01$). (L and M) Apoptotic cells in brains dissected from late-third-instar larvae were labeled with TdT (green). No significant cell death occurred in *c768–Gal4/UAS–Nop56^{RNAi}* brains (M). (N–O) Brains dissected from mid-third-instar larvae cultured at 25° were stained with Dpn and Dlg. (N1–N3) Three sections of a wild-type brain lobe, (N4) is a maximal projection (MP) image showing total Dpn$^+$ cells in the entire optic lobe. (O1–O3) Three sections of a *c768–Gal4/UAS–Nop56^{RNAi}* brain lobe; (O4) is a maximal projection image showing total Dpn$^+$ cells in the entire optic lobe. *Nop56* RNAi optic lobes had an increased number of Dpn$^+$ cells compared to wild type. Frontal view, lateral is to the left, medial to the right. Scale bar, 20 μm.

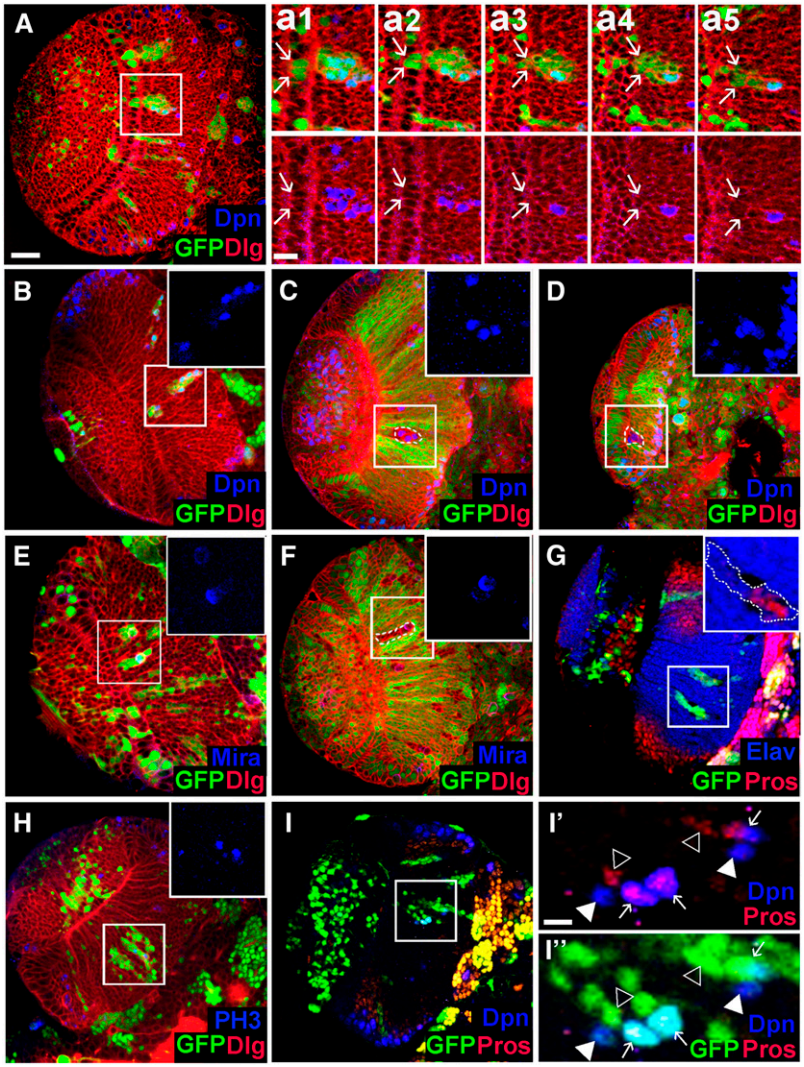

Figure 6 Loss of *Nop56* activity in cell clones leads to premature neuroepithelial differentiation into neuroblast. (A) A $Nop56^{RNAi}$ flip-out clone containing two to three NEs (indicated by arrows in a1 and a2) and a number of cells located in the medulla. a1–a5 show consecutive confocal sections of the mutant clone; arrows indicate the lateral edge of the clone. Several mutant cells in the medulla express Deadpan (Dpn). (B–D) Ectopic Dpn+ cells seen in $Nop56^{RNAi}$ clones (B) and $Nop56^{G4900}$ clones (C and D) entirely localized in the medulla. (E and F) Mutant cells in a $Nop56^{RNAi}$ clone (E) or a $Nop56^{G4900}$ clone (F) in the medulla undergo mitotic division with asymmetric polar localization of Miranda (Mira). (G) Mutant cells in a $Nop56^{RNAi}$ clone in the medulla express Prospero (Pros) or Elav. (H) Mutant cells in $Nop56^{RNAi}$ clones in the medulla undergo mitosis as detected by anti-phospho histone 3 (PH3) staining. (I, I′, I′′) Some Dpn+ cells in $Nop56^{RNAi}$ clones in the medulla express Prospero while other Dpn+ cells do not. Arrows in I′ and I′′ indicate coexpression of Dpn and Pros; arrowheads indicate expression of either Dpn or Pros. (A–I) Frontal view, lateral is to the left, medial to the right. Scale bar in A, 20 μm for A–I; scale bar in a1, 10 μm for a1–a5; scale bar in I′, 10 μm for I′ and I′′.

Loss of Nop56 accelerates lamina neurogenesis

The expression of *Nop56* RNAi using *c768–Gal4* caused defects in both medulla and lamina development (Figure 4, E and F), which could be attributed to a deficiency in neuroepithelial growth during the third-instar larval stages (Figure 5, E–H). When *Nop56* RNAi was induced by a different driver, *c855a–Gal4*, which is also expressed in the NEs from the first-instar stage onward (Figure 3N; Egger *et al.* 2007; Wang *et al.* 2011b), we found that although the medulla was somewhat smaller than wild type (Figure 7E; 92%, $n = 39$), the lamina was much enlarged (Figure 7F; 87%, $n = 39$); anti-Elav staining showed that more lamina cells had differentiated into neurons (Figure 7F′, 87%, $n = 39$). Several different $Nop56^{RNAi}$ constructs were tested; the expression of each construct caused an enlarged lamina (Figure S3). Enhanced lamina neurogenesis was also observed when *Nop56* RNA was knocked down at 25° (Figure 4, O and O′; compare with wild-type lamina in Figure 4, I and I′). *Nop56* RNAi using *c855a–Gal4* did not affect eye development (Figure S2C), indicating that lamina enlargement did not arise from abnormalities in the eye. These data indicate that reducing *Nop56* activity favors lamina neurogenesis. We noted that *Nop56* RNAi using *c855a–Gal4* consistently had a weaker effect on neuroepithelial growth than *Nop56* RNAi using *c768–Gal4* (compare Figure 4M with Figure 4J at 25°, and Figure 7D with Figure 4D at 31°), which may explain why we did not observe enlarged lamina in brains expressing $Nop56^{RNAi}$ using *c768–Gal4*; however, lamina cells that formed in such brains were all mature neurons (Figure 4F′ and L′), consistent with accelerated lamina neurogenesis seen in brains expressing $Nop56^{RNAi}$ under *c855a–Gal4* control.

Overexpression of Nop56 suppresses lamina neurogenesis

Since loss of *Nop56* function resulted in accelerated lamina neurogenesis, we tested whether *Nop56* overexpression may inhibit lamina neurogenesis. Indeed, overexpression of *Nop56* using *c855a–Gal4* suppressed lamina development. The lamina was reduced in size and there were very few mature lamina neurons (Figure 7, L and L′, 94%, $n = 16$).

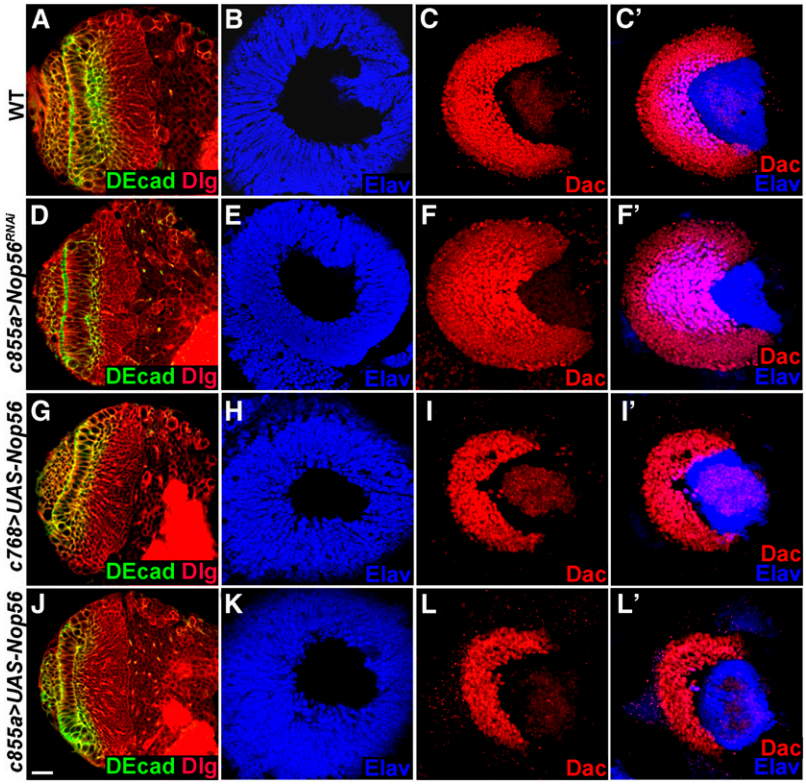

Figure 7 *Nop56* activity inhibits lamina neurogenesis. Brains dissected from late-third-instar larvae cultured at 31° were stained with the markers indicated. (A–C′) Wild-type optic lobes having columnar NEs (A), a dome-shaped medulla cortex (B), and a crescent lamina (C and C′). (D–F′) *c855a–Gal4/UAS–Nop56*^{RNAi} optic lobes having elongated NEs (D), and a smaller medulla (E), but a much enlarged lamina (F) with more mature lamina neurons (F′, Elav staining). (G–I′) Overexpression of *Nop56* using *c768–Gal4* caused a small lamina (I) and inhibited lamina neuron differentiation (I′, Elav staining), but did not affect medulla development (G and H). (J–L′) Overexpression of *Nop56* using *c855a–Gal4* caused a small lamina (L), and inhibited lamina neuron differentiation (L′, Elav staining), but had no effect on medulla development (J and K). (A, D, G, J) Frontal view, lateral is to the left, medial to the right; (B, C, C′, E, F, F′, H, I, I′, K, L, L′) lateral view, anterior is to the left, dorsal is up. Scale bar, 20 μm.

Nop56 overexpression did not appear to affect medulla development as judged by a normal size of the medulla cortex (Figure 7K, $n = 16$). Overexpression of *Nop56* using *c768–Gal4* also inhibited lamina development as reflected by a much smaller lamina with virtually no mature lamina neurons (Figure 7, I and I′, 85%, $n = 13$), and again no effect on medulla development was observed (Figure 7H, $n = 13$). We conclude that high *Nop56* activity suppresses lamina neuron differentiation.

Discussion

In this study, we have used genome-wide microarray assays to identify JAK/STAT target genes in the *Drosophila* brain. Forty-seven positively regulated genes have been identified. Many targets encode highly conserved proteins, which are excellent candidates for mediating JAK/STAT responses in mammalian brain development.

Several previous studies examined JAK/STAT targets in different tissues or cell types, including germ-line stem cells in the testis (Terry *et al.* 2006), eye imaginal discs (Flaherty *et al.* 2009), whole third-instar larvae (Kwon *et al.* 2008), and cultured Kc167 cells (Bina *et al.* 2010). Each of these studies compared differences between wild-type and JAK-activated mutants, and in each case, hundreds of potential targets were identified. Our study differs from the previous studies in that we examined not only JAK activated mutants but also, for the first time, JAK loss-of-function mutants. Thus, although we similarly identified hundreds of genes upregulated in JAK-activated brains (Figure 1H and Table S1), the JAK loss-of-function experiments allowed us to filter out a large number of genes that did not change expression in JAK-inactivated brains. Our approach was efficient since most of the candidate targets subsequently tested by *in situ* hybridization are indeed specifically expressed in the optic lobe, and all the targets positively responded to JAK signaling activity.

A comparison between our targets and those reported by Flaherty *et al.* (2009) and Terry *et al.* (2006) identified several common genes (Table 1 and Table 2). *terribly reduced optic lobes* (*trol*), which encodes a Perlecan, is the only positively regulated gene found in the eye disc, testis, and optic lobe, while several other targets in the optic lobe were found in either the eye disc or the testis. Notably, *chronologically inappropriate morphogenesis* (*chinmo*) is repressed by JAK/STAT in the optic lobe (Table 2), in contrast to it being activated in the eye disc and testis (Flaherty *et al.* 2009, 2010; Terry *et al.* 2006).

Conversely, several previously reported targets, namely, *Suppressor of cytokine signaling at 36E* (*SOCS36E*) (Karsten *et al.* 2002), *zinc finger homeodomain 1* (*Zfh-1*) (Terry *et al.* 2006; Leatherman and Dinardo 2008), *Protein tyrosine phosphatase 61F* (*PTP61F*) (Baeg *et al.* 2005; Muller *et al.* 2005), and *dome* (Ghiglione *et al.* 2002; Hombria *et al.* 2005; Rivas *et al.* 2008; Flaherty *et al.* 2009) were not identified in the optic lobe. Examination of their expression in the brains using antibody staining and quantitative PCR assays showed that these genes were not positively regulated by JAK/STAT in the optic lobe, as their expression either did not increase cell autonomously in JAK-activated brains (in the case of

SOCS36E, PTP61F, and Zfh-1) (Figure S4) or did not decrease in JAK-inactivated brains (in the case of *dome*) (Figure S5), although *SOCS36E* and *dome* total RNA did increase significantly in JAK-activated brains (Table S1 and Figure S5). Altogether, these results suggest that the JAK/STAT pathway may regulate different target genes in a tissue-specific manner.

JAK/STAT signaling and transcriptional control of gene expression

Our targets are enriched with transcription factors (Table 1). Strikingly, four of these genes are associated with Notch signaling. *E(spl)mδ*, *E(spl)m7*, and *Tom* are direct targets of the Notch pathway (Bray 2006), while H is a transcription corepressor involved in repression of Notch signaling activity (Bang *et al.* 1995). The Notch pathway is required for neuroepithelial maintenance and expansion (Egger *et al.* 2010; Ngo *et al.* 2010; Reddy *et al.* 2010; Yasugi *et al.* 2010; Orihara-Ono *et al.* 2011; Wang *et al.* 2011b; Weng *et al.* 2012). Our microarray data support a model in which JAK/STAT acts upstream of Notch signaling in the optic lobe (Wang *et al.* 2011a).

gcm and *gcm2* are both expressed in LPCs (Figure 2Q1; Chotard *et al.* 2005), and promote lamina neuron differentiation (Chotard *et al.* 2005). Although *gcm* and *gcm2* are activated by JAK/STAT (Figure 2Q2, Table 1), no STAT92E binding site clusters are identified in the noncoding genomic sequences of *gcm* or *gcm*. The JAK/STAT pathway may control their expression indirectly. Alternatively, STAT92E may utilize binding sites found somewhat further upstream of *gcm2* or downstream of *gcm* (not shown).

broad (*br*), *ftz transcription factor 1*(*ftz-f1*), *longitudinals lacking* (*lola*), *Oaz*, *vfl* (also called *Zelda*), and *CG10462* encode zinc finger transcription factors. *br*, *ftz-f1*, *lola*, *Oaz*, and *vfl* play diverse developmental roles in *Drosophila*; they each contain STAT92E binding site clusters in noncoding genomic sequences. It will be important to examine the roles of these zinc finger proteins in optic lobe development and their significance as effectors in mediating JAK/STAT activation.

Nop56 and optic lobe development

We have shown that *Nop56* is a functional downstream effector of STAT92E in the larval brain. The nucleolar localization of Nop56 suggests that like yeast Nop56p, Nop56 may be involved in ribosome synthesis and growth in *Drosophila*. Support for this role of Nop56 comes from the observation that RNAi knockdown of Fibrillarin, another component in the ribosomal RNA processing complex, caused very similar defects in neuroepithelial growth and lamina neurogenesis (Figure S6). The severe proliferation defects of $Nop56^{RNAi}$ mutant NEs might arise from retarded cellular growth. Paradoxically, $Nop56^{RNAi}$ mutant NEs became much elongated, suggesting an accumulation of cell mass. Perhaps *Nop56* RNAi did not entirely inhibit cellular growth while it blocked cell cycle progression. Nop56 activity is inhibitory to lamina neurogenesis at late larval stages. This effect is specific to the lamina, as the medulla was not affected by *Nop56* overexpression. We envision that cell growth is incompatible with neuron differentiation, and the loss of Nop56 activity might have accelerated the transition from LPCs to neurons.

Acknowledgments

We thank Drs. Erika Bach, Hugo Bellen, Chris Doe, Doug Harrison, Steve Hou, James Hombria, Yuh Nung Jan, Shigeaki Kato, Juergen Knoblich, Ruth Lehmann, Leonard Rabinow, and James Skeath for antibodies and fly stocks; the Bloomington Stock Center, the Tsinghua Stock Center, the National Institute of Genetics Stock Center, and the Vienna *Drosophila* RNAi Center for fly stocks; and the Developmental Studies Hybridoma Bank for antibodies. This work was supported by grants from the National Science Foundation of China (grant no. 30671035) and National Basic Sciences Research Programs (grant no. 2007CB947203) to H.L.

Literature Cited

Arbouzova, N. I., and M. P. Zeidler, 2006 JAK/STAT signalling in Drosophila: insights into conserved regulatory and cellular functions. Development 133: 2605–2616.

Bach, E. A., L. A. Ekas, A. Ayala-Camargo, M. S. Flaherty, H. Lee *et al.*, 2007 GFP reporters detect the activation of the Drosophila JAK/STAT pathway in vivo. Gene Expr. Patterns 7: 323–331.

Baeg, G. H., R. Zhou, and N. Perrimon, 2005 Genome-wide RNAi analysis of JAK/STAT signaling components in Drosophila. Genes Dev. 19: 1861–1870.

Bang, A. G., A. M. Bailey, and J. W. Posakony, 1995 Hairless promotes stable commitment to the sensory organ precursor cell fate by negatively regulating the activity of the Notch signaling pathway. Dev. Biol. 172: 479–494.

Bina, S., V. M. Wright, K. H. Fisher, M. Milo, and M. P. Zeidler, 2010 Transcriptional targets of Drosophila JAK/STAT pathway signalling as effectors of haematopoietic tumour formation. EMBO Rep. 11: 201–207.

Bray, S. J., 2006 Notch signalling: a simple pathway becomes complex. Nat. Rev. Mol. Cell Biol. 7: 678–689.

Chotard, C., W. Leung, and I. Salecker, 2005 *glial cells missing* and *gcm2* cell autonomously regulate both glial and neuronal development in the visual system of Drosophila. Neuron 48: 237–251.

Constantinescu, S. N., M. Girardot, and C. Pecquet, 2008 Mining for JAK-STAT mutations in cancer. Trends Biochem. Sci. 33: 122–131.

Copf, T., V. Goguel, A. Lampin-Saint-Amaux, N. Scaplehorn, and T. Preat, 2011 Cytokine signaling through the JAK/STAT pathway is required for long-term memory in Drosophila. Proc. Natl. Acad. Sci. USA 108: 8059–8064.

Egger, B., J. Q. Boone, N. R. Stevens, A. H. Brand, and C. Q. Doe, 2007 Regulation of spindle orientation and neural stem cell fate in the Drosophila optic lobe. Neural Dev. 2: 1.

Egger, B., K. S. Gold, and A. H. Brand, 2010 Notch regulates the switch from symmetric to asymmetric neural stem cell division in the Drosophila optic lobe. Development 137: 2981–2987.

Flaherty, M. S., J. Zavadil, L. A. Ekas, and E. A. Bach, 2009 Genome-wide expression profiling in the Drosophila eye reveals unexpected repression of Notch signaling by the JAK/STAT pathway. Dev. Dyn. 238: 2235–2253.

Flaherty, M. S., P. Salis, C. J. Evans, L. A. Ekas, A. Marouf *et al.*, 2010 *chinmo* is a functional effector of the JAK/STAT pathway that regulates eye development, tumor formation, and stem cell self-renewal in Drosophila. Dev. Cell 18: 556–568.

Furrer, M., M. Balbi, M. Albarca-Aguilera, M. Gallant, W. Herr *et al.*, 2010 Drosophila Myc interacts with host cell factor (dHCF) to activate transcription and control growth. J. Biol. Chem. 285: 39623–39636.

Gautier, T., T. Bergès, D. Tollervey, and E. Hurt, 1997 Nucleolar KKE/D repeat proteins Nop56p and Nop58p interact with Nop1p and are required for ribosome biogenesis. Mol. Cell. Biol. 17: 7088–7098.

Ghiglione, C., O. Devergne, E. Georgenthum, F. Carballes, C. Medioni *et al.*, 2002 The Drosophila cytokine receptor Domeless controls border cell migration and epithelial polarization during oogenesis. Development 129: 5437–5447.

Green, P., A. Y. Hartenstein, and V. Hartenstein, 1993 The embryonic development of the Drosophila visual system. Cell Tissue Res. 273: 583–598.

Harrison, D. A., R. Binari, T. S. Nahreini, M. Gilman, and N. Perrimon, 1995 Activation of a Drosophila Janus kinase (JAK) causes hematopoietic neoplasia and developmental defects. EMBO J. 14: 2857–2865.

Hayden, M. A., K. Akong, and M. Peifer, 2007 Novel roles for APC family members and Wingless/Wnt signaling during Drosophila brain development. Dev. Biol. 305: 358–376.

Hofbauer, A., and J. A. Campos-Ortega, 1990 Proliferation pattern and early differentiation of the optic lobes in *Drosophila melanogaster*. Rouxs Arch. Dev. Biol. 198: 264–274.

Hombría, J. C., S. Brown, S. Häder, and M. P. Zeidler, 2005 Characterisation of Upd2, a Drosophila JAK/STAT pathway ligand. Dev. Biol. 288: 420–433.

Hulf, T., P. Bellosta, M. Furrer, D. Steiger, D. Svensson *et al.*, 2005 Whole-genome analysis reveals a strong positional bias of conserved dMyc-dependent E-boxes. Mol. Cell. Biol. 25: 3401–3410.

Jiang, H., P. H. Patel, A. Kohlmaier, M. O. Grenley, D. G. McEwen *et al.*, 2009 Cytokine/Jak/Stat signaling mediates regeneration and homeostasis in the Drosophila midgut. Cell 137: 1343–1355.

Johnson, A. N., M. H. Mokalled, T. N. Haden, and E. N. Olson, 2011 JAK/Stat signaling regulates heart precursor diversification in Drosophila. Development 138: 4627–4638.

Karsten, P., S. Häder, and M. P. Zeidler, 2002 Cloning and expression of Drosophila SOCS36E and its potential regulation by the JAK/STAT pathway. Mech. Dev. 117: 343–346.

Kunes, S., 2000 Axonal signals in the assembly of neural circuitry. Curr. Opin. Neurobiol. 10: 58–62.

Kwon, S. Y., H. Xiao, B. P. Glover, R. Tjian, C. Wu *et al.*, 2008 The nucleosome remodeling factor (NURF) regulates genes involved in Drosophila innate immunity. Dev. Biol. 316: 538–547.

Lacronique, V., A. Boureux, V. D. Valle, H. Poirel, C. T. Quang *et al.*, 1997 A TEL-JAK2 fusion protein with constitutive kinase activity in human leukemia. Science 278: 1309–1312.

Leatherman, J. L., and S. DiNardo, 2008 Zfh-1 controls somatic stem cell self-renewal in the Drosophila testis and nonautonomously influences germline stem cell self-renewal. Cell Stem Cell 3: 44–54.

Levy, D. E., J. E. Darnell, Jr., 2002 Stats: transcriptional control and biological impact. Nat. Rev. Mol. Cell Biol. 3: 651–662.

Liu, W., S. R. Singh, and S. X. Hou, 2010 JAK-STAT is restrained by Notch to control cell proliferation of the Drosophila intestinal stem cells. J. Cell. Biochem. 109: 992–999.

Luo, W., and A. Sehgal, 2012 Regulation of circadian behavioral output via a microRNA-JAK/STAT circuit. Cell 148: 765–779.

Luo, H., W. P. Hanratty, and C. R. Dearolf, 1995 An amino acid substitution in the Drosophila $hop^{Tum\text{-}l}$ Jak kinase causes leukemia-like hematopoietic defects. EMBO J. 14: 1412–1420.

Meinertzhagen, I. A., and T. E. Hanson, 1993 The development of the optic lobe, pp. 1363–1491 in *The Development of Drosophila melanogaster*, edited by M. Bate, and A. Martinez-Arias. Cold Spring Harbor Laboratory Press, Cold Spring Harbor, NY.

Mohanty, S., K. A. Jermyn, A. Early, T. Kawata, L. Aubry *et al.*, 1999 Evidence that the Dictyostelium Dd-STATa protein is a repressor that regulates commitment to stalk cell differentiation and is also required for efficient chemotaxis. Development 126: 3391–3405.

Muller, P., D. Kuttenkeuler, V. Gesellchen, M. P. Zeidler, and M. Boutros, 2005 Identification of JAK/STAT signalling components by genome-wide RNA interference. Nature 436: 871–875.

Murata, T., E. Suzuki, S. Ito, S. Sawatsubashi, Y. Zhao *et al.*, 2008 RNA-binding protein hoip accelerates polyQ-induced neurodegeneration in Drosophila. Biosci. Biotechnol. Biochem. 72: 2255–2261.

Nassif, C., A. Noveen, and V. Hartenstein, 2003 Early development of the Drosophila brain: III. The pattern of neuropile founder tracts during the larval period. J. Comp. Neurol. 455: 417–434.

Neumüller, R. A., C. Richter, A. Fischer, M. Novatchkova, K. G. Neumüller *et al.*, 2011 Genome-wide analysis of self-renewal in Drosophila neural stem cells by transgenic RNAi. Cell Stem Cell 8: 580–593.

Ngo, K. T., J. Wang, M. Junker, S. Kriz, G. Vo *et al.*, 2010 Concomitant requirement for Notch and Jak/Stat signaling during neuro-epithelial differentiation in the Drosophila optic lobe. Dev. Biol. 346: 284–295.

Orian, A., B. van Steensel, J. Delrow, H. J. Bussemaker, L. Li *et al.*, 2003 Genomic binding by the Drosophila Myc, Max, Mad/Mnt transcription factor network. Genes Dev. 17: 1101–1114.

Orihara-Ono, M., M. Toriya, K. Nakao, and H. Okano, 2011 Downregulation of Notch mediates the seamless transition of individual Drosophila neuroepithelial progenitors into optic medullar neuroblasts during prolonged G1. Dev. Biol. 351: 163–175.

O'Shea, J. J., M. Gadina, and R. D. Schreiber, 2002 Cytokine signaling in 2002: new surprises in the Jak/Stat pathway. Cell 109 (Suppl.): S121–S131.

Pierce, S. B., C. Yost, S. A. R. Anderson, E. M. Flynn, J. Delrow *et al.*, 2008 Drosophila growth and development in the absence of dMyc and dMnt. Dev. Biol. 315: 303–316.

Reddy, B. V., C. Rauskolb, and K. D. Irvine, 2010 Influence of Fat-Hippo and Notch signaling on the proliferation and differentiation of Drosophila optic neuroepithelia. Development 137: 2397–2408.

Rivas, M. L., L. Cobreros, M. P. Zeidler, and J. C. Hombría, 2008 Plasticity of Drosophila Stat DNA binding shows an evolutionary basis for Stat transcription factor preferences. EMBO Rep. 9: 1114–1120.

Struhl, G., and K. Basler, 1993 Organizing activity of wingless protein in Drosophila. Cell 72: 527–540.

Tautz, D., and C. Pfeifle, 1989 A non-radioactive in situ hybridization method for the localization of specific RNAs in Drosophila embryos reveals translational control of the segmentation gene hunchback. Chromosoma 98: 81–85.

Terry, N. A., N. Tulina, E. Matunis, and S. DiNardo, 2006 Novel regulators revealed by profiling Drosophila testis stem cells within their niche. Dev. Biol. 294: 246–257.

Wang, W., Y. Li, L. Zhou, H. Yue, and H. Luo, 2011a Role of JAK/STAT signaling in neuroepithelial stem cell maintenance and proliferation in the Drosophila optic lobe. Biochem. Biophys. Res. Commun. 410: 714–720.

Wang, W., W. Liu, Y. Wang, L. Zhou, X. Tang *et al.*, 2011b Notch signaling regulates neuroepithelial stem cell maintenance and neuroblast formation in Drosophila optic lobe development. Dev. Biol. 350: 414–428.

Weng, M., J. M. Haenfler, and C. Y. Lee, 2012 Changes in Notch signaling coordinates maintenance and differentiation of the Drosophila larval optic lobe neuroepithelia. Dev. Neurobiol. 72: 1376–1390.

Xu, N., S. Q. Wang, D. Tan, Y. Gao, G. Lin *et al.*, 2011 EGFR, Wingless and JAK/STAT signaling cooperatively maintain Drosophila intestinal stem cells. Dev. Biol. 354: 31–43.

Yan, R., S. Small, C. Desplan, C. R. Dearolf, and J. E. Darnell, Jr., 1996 Identification of a *Stat* gene that functions in Drosophila development. Cell 84: 421–430.

Yasugi, T., D. Umetsu, S. Murakami, M. Sato, and T. Tabata, 2008 Drosophila optic lobe neuroblasts triggered by a wave of proneural gene expression that is negatively regulated by JAK/STAT. Development 135: 1471–1480.

Yasugi, T., A. Sugie, D. Umetsu, and T. Tabata, 2010 Coordinated sequential action of EGFR and Notch signaling pathways regulates proneural wave progression in the Drosophila optic lobe. Development 137: 3193–3203.

Zhou, L., and H. Luo, 2013 Replication protein A links cell cycle progression and the onset of neurogenesis in Drosophila optic lobe development. J. Neurosci. 33: 2873–2888.

Communicating editor: I. K. Hariharan

GENETICS

Supporting Information
http://www.genetics.org/lookup/suppl/doi:10.1534/genetics.113.155945/-/DC1

Evidence for Tissue-Specific JAK/STAT Target Genes in *Drosophila* Optic Lobe Development

Hongbin Wang, Xi Chen, Teng He, Yanna Zhou, and Hong Luo

DOI: 10.1534/genetics.113.155945

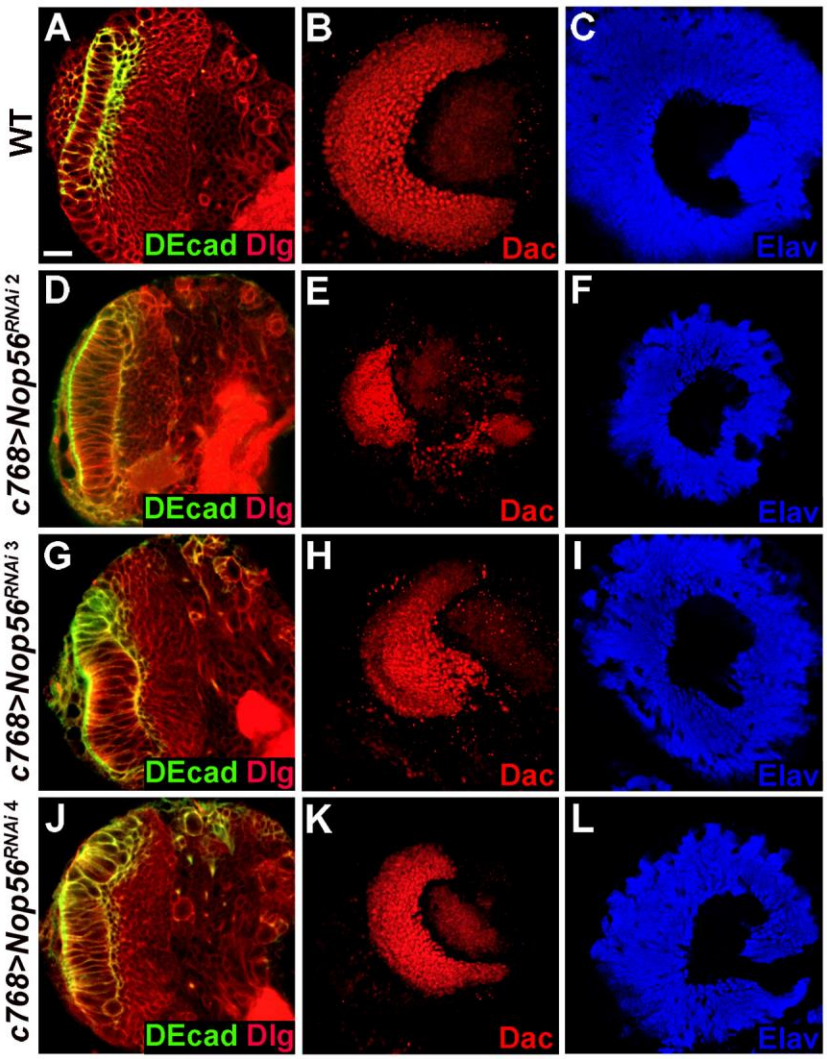

Figure S1 *Nop56* RNAi knockdown causes defects in medulla and lamina development. Brains dissected from late-third instar larvae cultured at 31° were stained with the markers indicated. Three different *UAS-Nop56^{RNAi}* constructs were expressed using *c768-Gal4*. Expression of these RNAi constructs inhibited neuroepithelial proliferation, resulting in elongated NEs (D, G, J), smaller lamina (E, H, K), and smaller medulla (F, I, L), compared to wild type (A-C). (A, D, G, J) Frontal view, lateral is to the left, medial to the right; (B, C, E, F, H, I, K, L) lateral view, anterior is to the left, dorsal is up. Scale bar: 20μm.

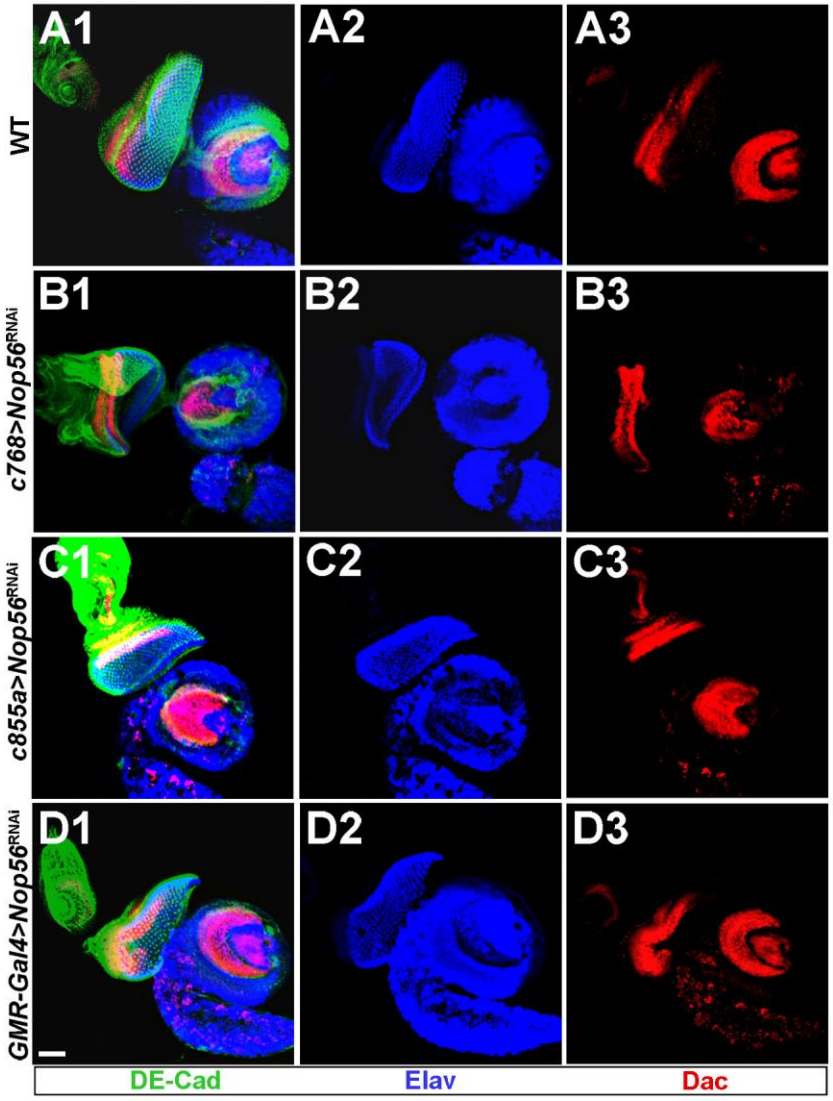

Figure S2 The defects in *Nop56* RNAi optic lobes do not result from the eye. Brain lobes with attached eye imaginal discs were dissected from late-third instar larvae cultured at 31°, and stained with the markers indicated. (A) Wild type eye disc and optic lobe. (B) *c768-Gal4/UAS-Nop56^{RNAi}* eye disc having a normal number of differentiated photoreceptors (B1, B2) projected to a smaller lamina (B3). (C) *c855a-Gal4/UAS-Nop56^{RNAi}* eye disc having a normal number of differentiated photoreceptors (C1, C2) projected to an enlarged lamina (C3). (D) *GMR-Gal4/UAS-Nop56^{RNAi}* eye disc and optic lobe developed normally. Lateral view, anterior is to the left, dorsal is up. Scale bar: 40μm.

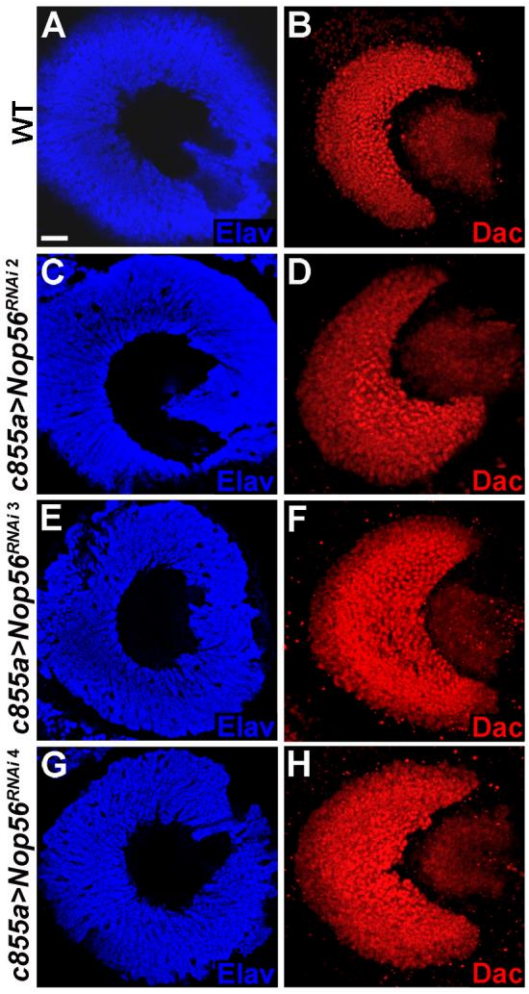

Figure S3 *Nop56* RNAi enhances lamina neurogenesis. Brains dissected from late-third instar larvae cultured at 31° were stained with Elav and Dac. (A, B) Wild type medulla (A) and lamina (B); (C-H) The expression of three different *UAS-Nop56^{RNAi}* constructs using *c855a-Gal4* led to enlarged lamina (D, F, H) as compared with wild type (B). Lateral view, anterior is to the left, dorsal is up. Scale bar: 20μm.

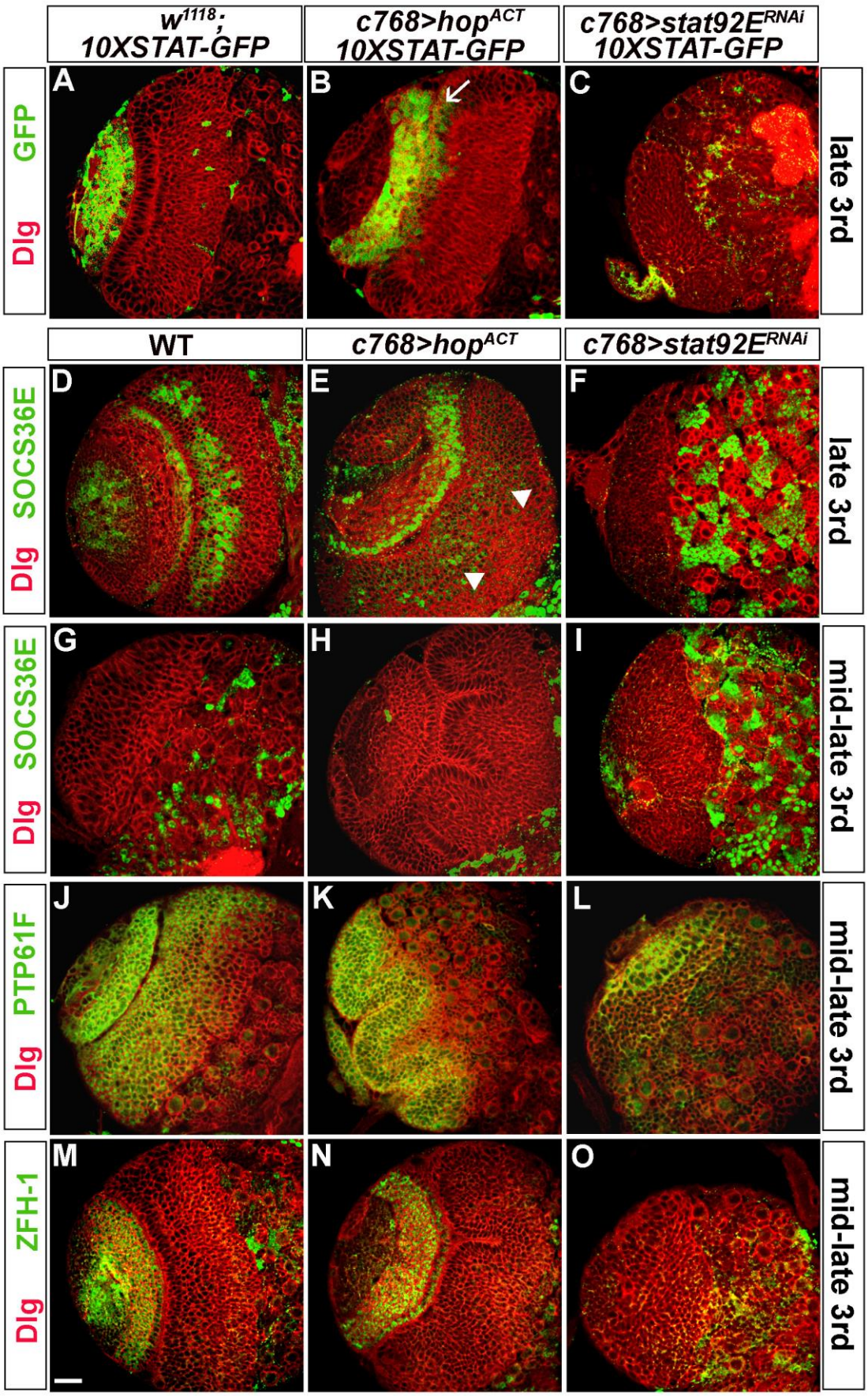
w1118; 10XSTAT-GFP
c768>hopACT 10XSTAT-GFP
c768>stat92ERNAi 10XSTAT-GFP
Dlg GFP
A
B
C
late 3rd
WT
c768>hopACT
c768>stat92ERNAi
Dlg SOCS36E
D
E
F
late 3rd
Dlg SOCS36E
G
H
I
mid-late 3rd
Dlg PTP61F
J
K
L
mid-late 3rd
Dlg ZFH-1
M
N
O
mid-late 3rd

Figure S4 Expression of previously reported targets in the optic lobe. Brains from late-third instar (A-F) or mid-late third instar larvae (G-O) cultured at 25^{o} were stained with the markers indicated. (A-C) The *10XSTAT92E-GFP* reporter is strongly expressed in the lamina, but virtually undetectable in the NEs (A); the reporter expression weakly increased in the NEs of JAK activated brains (B, indicated by arrow), but was not detectable in JAK inactivated brains which had no NEs (C). (D-F) At late-third instar, SOCS36E protein is strongly expressed in the NEs, medulla neuroblasts, LPCs, and some developing lamina neurons, as well as strongly expressed in neurons of the central brain (D). SOCS36E expression did not increase cell autonomously in the NEs of JAK activated brains (E, arrowheads indicate SOCS36E expression in the overgrown neuroepithelium), but was undetectable in JAK inactivated brains which essentially lost all NEs (F). (G-I) At mid-late third instar, SOCS36E protein is not expressed in the optic lobe, but is strongly expressed in neurons and neuroblasts of the central brain. (J-L) PTP61F is strongly expressed in the NEs, medulla neuroblasts, LPCs, and the lamina, and is also expressed in central brain neuroblasts (J); PTP61F expression did not appear to increase cell autonomously in the NEs and lamina cells of JAK activated brains (K), and was not reduced in the residual NEs of JAK inactivated brains (L). (M-O) Zfh-1 protein is expressed in the lamina (M); Zfh-1 expression did not increase in JAK activated brains (N), but was undetectable in JAK inactivated brains which had no lamina (O). Frontal view, lateral is to the left, medial to the right. Scale bar: 20μm.

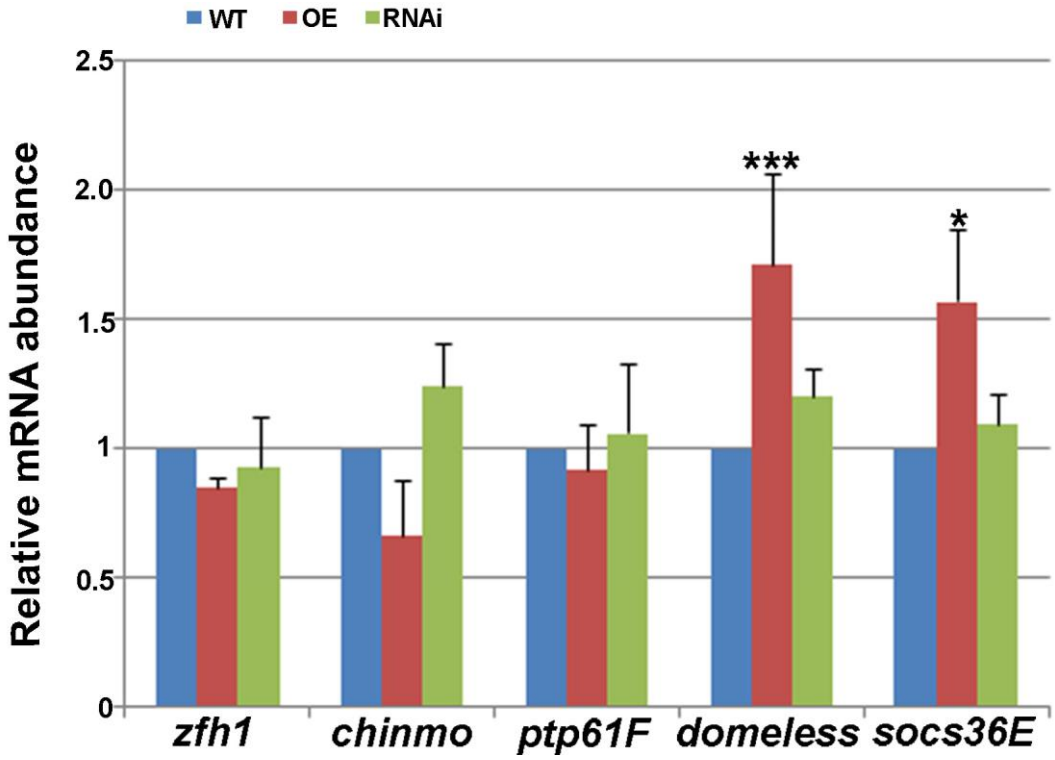

Figure S5 Relative expression levels of previously reported targets determined by quantitative PCR. Total RNAs were isolated from the CNS of late-third instar larvae cultured at 25°; reversed transcribed cDNAs were used as template in PCR using the SYBR Green PCR Master mix (Applied Biosystems). The signals were normalized to the internal reference, ribosome protein 49-encoding gene (*Rp49*). The PCR was run in triplicates per primer set, and repeated 4 independent times. *Zfh-1* and *PTP61F* RNA levels did not change in JAK activated or inactivated brains; *domeless* and *SOCS36E* RNA levels significantly increased in JAK activated brains, but did not decrease in JAK inactivated brains; *chinmo* expression was repressed by JAK signaling, although not statistically significant. WT: wild type; OE: *c768-Gal4/UAS-hop*$^{Tum\text{-}l}$; RNAi: *c768-Gal4/UAS-stat92E*^{RNAi}. ***: p <0.01; *: p<0.05.

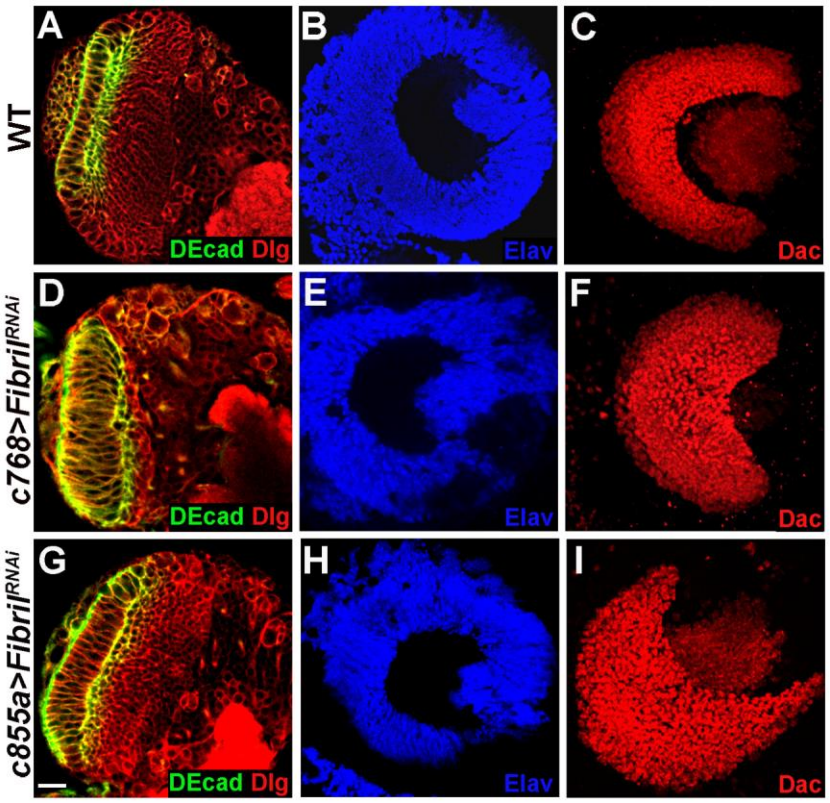

Figure S6 *Fibrillarin* RNAi causes defects in lamina and medulla development. Brains dissected from late-third instar larvae cultured at 31^{o} were stained with the markers indicated. (A-C) Wild type brains. (D-F) Expression of *Fibrillarin^{RNAi}* using *c768-Gal4* inhibited neuroepithelial proliferation, resulting in elongated NEs (D, 87%, n=32), a smaller medulla (E, 72%, n=29), and an enlarged lamina (F, 86%, n=29). (G-I) Expression of *Fibrillarin^{RNAi}* using *c855a-Gal4* weakly inhibited neuroepithelial proliferation, resulting in somewhat elongated NEs (G, 78%, n=27), slightly smaller medulla (H, 79%, n=21), and enlarged lamina (I, 95%, n=21). (A, D, G) Frontal view, lateral is to the left, medial to the right; (B, C, E, F, H, I) lateral view, anterior is to the left, dorsal is up. Scale bar: 20μm.

Tables S1-S2 are available for download at http://www.genetics.org/lookup/suppl/doi:10.1534/genetics.113.155945/-/DC1

Table S1 Genes up or down regulated in *upd*-overexpressing brains

Table S2 Genes down or up regulated in hop^{M4} brains